

Revised submission to ApJ

Radial Velocities for 889 Late-type Stars¹

David L. Nidever², Geoffrey W. Marcy^{2,3}, R. Paul Butler⁴, Debra A. Fischer³, Steven S. Vogt⁵

dnidever@stars.sfsu.edu

ABSTRACT

We report radial velocities for 844 FGKM-type main sequence and subgiant stars and 45 K giants, most of which had either low-precision velocity measurements or none at all. These velocities differ from the standard stars of Udry et al. (1999a) by 0.035 km s⁻¹ (RMS) for the 26 FGK standard stars in common. The zero-point of our velocities differs from that of Udry et al.: $\langle V_{\text{present}} - V_{\text{Udry}} \rangle = +0.053$ km s⁻¹. Thus these new velocities agree with the best known standard stars both in precision and zero-point, to well within 0.1 km s⁻¹.

Nonetheless, both these velocities and the standards suffer from three sources of systematic error, namely, convective blueshift, gravitational redshift, and spectral type mismatch of the reference spectrum. These systematic errors are here forced to be zero for G2V stars by using the Sun as reference, with Vesta and day sky as proxies. But for spectral types departing from solar, the systematic errors reach 0.3 km s⁻¹ in the F and K stars and 0.4 km s⁻¹ in M dwarfs.

Multiple spectra were obtained for all 889 stars during four years, and 782 of them exhibit velocity scatter less than 0.1 km s⁻¹. These stars may serve as radial velocity standards if they remain constant in velocity. We found 11 new spectroscopic binaries and report orbital parameters for them.

¹Based on observations obtained at the W.M. Keck Observatory, which is operated jointly by the University of California and the California Institute of Technology, and on observations obtained at the Lick Observatory which is operated by the University of California.

²Department of Physics and Astronomy, San Francisco State University, San Francisco, CA USA 94132

³Department of Astronomy, University of California, Berkeley, CA USA 94720

⁴Department of Terrestrial Magnetism, Carnegie Institution of Washington, 5241 Broad Branch Road NW, Washington DC, USA 20015-1305

⁵UCO/Lick Observatory, University of California at Santa Cruz, Santa Cruz, CA, USA 95064

Subject headings: stars: fundamental parameters; late-type; kinematics – techniques: radial velocities; spectroscopic – catalogs; binaries: spectroscopic

1. Introduction

The radial velocity of a star is ideally the component of the velocity vector of its center of mass that lies along the line-of-sight. Radial velocities are valuable for a variety of astrophysical investigations, including studies of the structure of the Milky Way Galaxy, the orbits of long-period binary stars, and the distances to star clusters (see for example, Binney and Merrifield (1998)). “Barycentric” radial velocities (sometimes referred to as “absolute” radial velocities), such as reported here, are measured relative to the barycenter, or center of mass, of the Solar System. Such velocities are often (incorrectly) termed “heliocentric”, though the Sun moves with a speed of $\sim 13 \text{ m s}^{-1}$ relative to the barycenter.

Radial velocities of stars in the Galaxy are often measured with an accuracy of only $\sim 0.5 \text{ km s}^{-1}$. With advances in the accuracy of proper motion measurements to $\sim 1 \text{ mas/yr}$ (e.g., Perryman et al. 1996) for many stars, a corresponding increase in the accuracy of radial velocities is required. Meanwhile, the best *relative* radial velocities have precisions of 3 m s^{-1} (Butler et al. 2000) and new instruments (e.g. HARPS) are designed to achieve a precision of 1 m s^{-1} (Bouchy et al. 2001; Pepe et al. 2000). These relative velocities have proved useful in the detection of extrasolar planets (e.g., Marcy, Cochran, & Mayor (2000)) but they are not necessarily tied to a velocity zero-point. Nonetheless, the precision–velocity instruments have overcome many observational and technical hurdles related to spectroscopic Doppler–shift measurements, either by using a gas absorption cell or a fiber–fed comparison lamp spectrum (Valenti et al. 1995; Butler et al. 1996; Baranne 2000).

The precision–velocity technology has been applied to the establishment of barycentric radial velocities, most notably by the Geneva team (Udry et al. 1999a,b). They have measured velocities for 38 stable dwarf stars with precision better than 0.05 km s^{-1} .

Here we provide barycentric radial velocities with typical accuracies of 0.3 km s^{-1} (and precise to 0.03 km s^{-1} for a given spectral type) for 889 stars. Our intent is to provide a velocity measurement at the current epoch for a variety of purposes. Velocity variations with a time scale of hundreds of years may be detected by comparison of present and future velocities. We also hope to establish radial velocity standard stars, by indentifying a subset that exhibit no significant velocity variation above 10 m s^{-1} .

2. Barycentric Radial Velocities

The Doppler searches for planets have been successful because of the relative ease with which the change in radial velocity may be measured with high internal precision. Such relative velocities circumvent the technical challenges associated with the determination of an accurate velocity zero-point and they avoid the physical interpretation of a barycentric Doppler shift which becomes bewildering at levels below 1 km s^{-1} .

Barycentric Doppler shifts carry an unclear interpretation for several reasons. Stellar lines suffer a gravitational redshift (Misner, Thorne, & Wheeler 1973) upon leaving the stellar photosphere, yielding effective redshifts of $V_{\text{grav}} = GM/Rc$ (Dravins et al. 1999). This redshift varies from 680 m s^{-1} for F5V to 500 m s^{-1} for M5V stars, the range of spectral types considered here. Uncertainties in stellar masses and radii prevent an accurate removal of this effect. Furthermore, stellar lines suffer a transverse Doppler effect (essentially time dilation), the removal of which requires knowledge of the full velocity vector of the star's space motion. This effect is $\simeq 50 \text{ m s}^{-1}$ for the fastest moving stars (Lindegren et al. 1999).

More importantly, stellar Doppler shifts are affected by sub-photospheric convection (granulation), macro-turbulence, stellar rotation, pressure shifts, oscillations and activity cycles. The most important of these effects is granulation. The textbook explanation is that a larger contribution to the stellar flux emerges from hot, rising gas than from falling gas in the convective cells. These motions yield an overall blueshift of spectral lines (Dravins 1999). However, the exact convective blueshift depends on the full 3-D hydrodynamics and radiative transfer in each spectral line as a function of depth in the photosphere (Dravins 1999). The blueshift clearly depends on spectral type and is expected to be $\sim -1000 \text{ m s}^{-1}$ for F5V, -400 m s^{-1} for G2V, and -200 m s^{-1} for K0V (Dravins et al. 1999). Effects due to pressure shifts are less than 100 m s^{-1} for ordinary stars (Dravins et al. 1999; Allende Prieto et al. 1997). Stellar rotation also imposes minor radial velocity effects (Gray 1999).

Moreover, the measurement of spectroscopic barycentric radial velocities usually requires a reference stellar spectrum. Due to constraints of telescope time and available standard stars, only a small number of reference spectra can be used. Typically, the Doppler measurements require use of reference spectra having different spectral types than the program star, which leads to spectral mismatch errors. Since the strengths of spectral lines vary with temperature and metalicity, the spectra of the reference and program stars will be significantly different. In effect, the relative displacement in wavelength between two non-identical spectra is not uniquely defined and therefore is dependent on the algorithm used. Such spurious Doppler effects are minimized, but not eliminated, by using high-resolution spectra with many lines resolved, as adopted in this present survey.

The effects of convection, stellar gravitational redshift, transverse Doppler shift, and the other effects mentioned above cannot be determined for a star with an accuracy that is comparable to the internal measurement errors of $\sim 10 \text{ m s}^{-1}$. Removal of such effects by a model of each star might introduce more model-dependent errors. Nonetheless, with considerable modeling, the measurement of a Doppler shift may be used to determine the “true” velocity component of the center of mass of the star. Alternatively (and more traditionally) Doppler measurements may be left merely as an observable, namely the spectroscopic shift in wavelength, often quoted as $z = \Delta\lambda/\lambda_0$ (Lindegren et al. 1999).

Here, we adopt the philosophy that spectroscopic barycentric radial velocities should first be corrected for local effects, such as that caused by the observer’s motion relative to the Solar System barycenter ($\sim 30 \text{ km s}^{-1}$) and by the solar gravitational blueshift ($\sim 3 \text{ m s}^{-1}$). In addition, we will correct all of our velocities of FGK stars for gravitational redshift and convective blueshift to first order by using the known radial velocity of the Sun to set the zero-point for the stellar velocity measurements.

Our quoted Doppler shifts represent velocities as if measured at the Solar System barycenter but with the Sun and its potential well removed. Clearly the velocity measurements presented here are amenable to future corrections for the spectral-type dependence relative to G2V for gravitational redshift and convective blueshift, in order to yield the most accurate velocities possible for them (e.g., Gullberg (1999); Saar & Fischer (2000)).

3. Spectroscopic Observations

The spectra were obtained with the HIRES echelle spectrometer (Vogt et al. 1994) on the 10-m Keck 1 telescope and with the “Hamilton” echelle spectrometer fed by either the 3-m Shane or the 0.6-m Coude Auxilliary (CAT) Telescopes (Vogt 1987). During an observation the starlight is sent through a glass cell that is filled with iodine vapor (Marcy & Butler 1992) before entering the spectrometer, which superimposes iodine lines on the stellar lines. These iodine absorption lines are used to calibrate the wavelength scale of the spectrum from 5000 Å–6000 Å.

Our Doppler planet search project contains 889 stars at the Keck and Lick Observatories (Butler et al. 2000). Until now only relative radial velocities have been computed from these spectra and they have a precision of $\sim 3 \text{ m s}^{-1}$ (Butler et al. 1996; Vogt et al. 2000) which has allowed the discovery of Jovian and sub-Jovian sized extrasolar planets (Marcy, Cochran, & Mayor 2000).

To achieve barycentric velocities, we adopt two standard spectra. We use the National

Solar Observatory (NSO) FTS solar spectrum (Kurucz et al. 1984) and an M dwarf composite spectrum (see §4) as reference spectra. The 889 stars each typically have \sim 12 spectra obtained during four years from 1997 to 2001. The distribution of spectral types in our sample is: 14% F, 46% G, 27% K, and 13% M stars. Except for 45 K giants all stars are main-sequence dwarfs or subgiants. All stars are void of a visible companion within 2 arcsec, though some were subsequently revealed to be spectroscopic binaries (see §9).

4. Doppler Method

The barycentric radial velocities reported here are found in a manner similar to that used to find the relative radial velocities for the planet search. An observed spectrum is fit with a synthetic spectrum that is composed of the individual stellar and iodine spectra. In detail, the synthetic spectrum is the product of the deconvolved stellar “template” spectrum (with the spectrometer instrumental profile removed) with a high resolution spectrum of molecular iodine. The product of these two is convolved with the instrumental profile of the spectrometer (at the time of the observation), to produce the final synthetic spectrum, as described in Butler et al. (2000).

The observed spectrum to be synthesized is broken into ”chunks” of length 40 pixels corresponding to roughly \sim 2 Å. In total 14 free parameters are fit in the Doppler analysis; 11 devoted to the instrumental profile, along with the wavelength zero-point of each chunk, the wavelength dispersion across each chunk, and the Doppler shift of the stellar spectrum relative to the stellar template of that star, z ($= \Delta\lambda/\lambda$). All of the parameters, except for z , are extracted primarily from the iodine portion of the observed spectrum. After the best parameters are found for all the chunks of a spectrum they are saved for further analysis, notably the weighted average of z . We apply a correction to all velocities for our topocentric motion relative to the barycenter (McCarthy 1995). For a more in depth discussion of this standard Doppler analysis to obtain relative velocities, see Marcy & Butler (1992); Butler et al. (1996); Valenti et al. (1995).

To obtain barycentric radial velocities, the approach was similar to the standard analysis described above and indeed we used some parameters derived from that analysis. Here, we used the National Solar Observatory (NSO) solar spectrum (Kurucz et al. 1984) as the deconvolved template, for all F, G and K stars. For M dwarfs, we constructed an in-house M star composite spectrum as the template (see below). Since all parameters except for z are extracted from the iodine portion of the spectrum previously, the use of a different stellar template spectrum does not affect these parameters significantly. Therefore in our new fit, we simply adopt the values of the 13 non- z parameters that were previously obtained in the

Doppler analysis for relative velocities (i.e., for the planet search) and we fit here only for the barycentric radial velocity, z .

Ordinarily, when the deconvolved stellar spectrum of the individual star is used as the template, the χ^2_ν statistic is near unity (usually less than 1.7), because the stellar contribution to the model is a previously obtained deconvolved spectrum of the same star. But in our fit for barycentric velocities, the value of reduced χ^2_ν is much larger (poorer) because of the mismatch between the template spectrum (NSO or M dwarf composite) and that of the program star. The program star differs from the Solar or M-dwarf template in spectral type, metalicity, and $v \sin i$. Thus, the spectral fits are not as good, yielding χ^2_ν of 3–7.

The internal error per observation, as defined by the weighted standard deviation of the mean of the velocities from all (~ 400) chunks, is higher for our barycentric radial velocities than for the relative radial velocities used in the planet search. We find that while the relative velocities carry errors of $\sim 3 \text{ m s}^{-1}$ (for the planet search) the average internal error per observation for the barycentric velocities reported here is $\sim 20 \text{ m s}^{-1}$. A more conservative estimate of our velocity precision is given in §6 as 0.03 km s^{-1} from comparison with the standard stars.

Due to the fact that only one stellar template is used for a large range of stellar types, we expect that our errors (internal error per observation) will depend on $B-V$. The greater the difference between template and program star, the greater the expected error due to spectral mismatch. We plot this internal error in our barycentric velocities versus $B-V$ in Figure 1. Since the NSO solar spectrum, $B-V = 0.64$ (Carroll and Ostlie 1996), is used for F, G and K stars we expect the errors to be minimized for solar type stars. This is confirmed in Figure 1. The M dwarf composite template spectrum was created from five different M dwarfs having average spectral type of M3 (see below). The internal velocity errors for stars analyzed with this stellar template are minimized at $B-V \approx 1.5$, as can also be seen in Figure 1.

Each program star has an average of 12 observations. As many observations as possible are analyzed per star, up to 30, in order to minimize the uncertainty in the mean of the barycentric radial velocities. If the radial velocity of the star were stable we should obtain an uncertainty in the mean of $\sim 20/\sqrt{12} \approx 6 \text{ m s}^{-1}$. A majority of stars indeed exhibit velocity scatter of $\sim 10 \text{ m s}^{-1}$ (RMS) while others have an RMS scatter larger than 100 m s^{-1} . Scatter in the latter stars is almost always caused by companions or large chromospheric activity. Overall, 782 of the 889 stars have an RMS velocity scatter less than 0.1 km s^{-1} , and 107 stars have an RMS velocity scatter larger than 0.1 km s^{-1} . The barycentric radial velocities for these stars are reported in Tables 1 and 2 respectively.

As mentioned above, the NSO solar spectrum could not be used as the template for the M dwarf program stars because the spectra are too different. Therefore, a separate reference spectrum was required for the M stars. For this purpose a composite spectrum of five M stars was produced in the following manner.

Five M stars were selected having barycentric radial velocities reported by Marcy et al. (1987) with low uncertainties: GJ 251 (M4), GJ 411 (M2), GJ 526 (M4), GJ 752A (M3.5), and GJ 908 (M2). One spectrum of high S/N ratio was used from each of these M dwarfs. The spectra were shifted back, to remove the Doppler shifts caused by the barycentric motion of the observatory and by the barycentric radial velocity of the star itself relative to the barycenter, taken from Marcy et al. (1987). To check for any residual Doppler shifts, these corrected spectra were then cross-correlated with respect to one of them, GJ 251. Assuming the resulting displacements were due to random errors, the mean of the residual velocities was taken to be the barycentric velocity zero-point. Using this reference point the spectra were again corrected for their doppler shifts. Finally, the spectra were put on the same wavelength scale and coadded to create a M star composite spectrum.

5. Velocity Zero-Point

Using observations of the day sky and the minor planet Vesta we found the zero-point of our velocities for FGK stars. These references were used because they have essentially solar spectra, and the radial velocities of Vesta and the sun relative to a topocentric observer are easily determined. We used the online “JPL Ephemeris Generator” to find these instantaneous velocities⁶. Four observations of the day sky and two observations of Vesta were analysed with the before mentioned Doppler method using the NSO solar spectrum. These references showed that our raw velocities, from Keck and Lick, were consistently large by $522 \pm 5 \text{ m s}^{-1}$.

There are various possible sources for the 522 m s^{-1} offset in our raw velocities. The absolute wavelength scales of both the NSO solar spectrum and our FTS iodine spectrum are not well known. According to Kurucz et al. (1984), the solar lines are broadened by 200 m s^{-1} due to the change in the radial velocity during the observation, and the wavelengths may have errors as large as 100 m s^{-1} . The wavelength scale of the iodine FTS spectrum comes from the calibration made at the McMath telescope at Kitt Peak. We have no independent way to verify the integrity of the zero-point in wavelength of this FTS iodine spectrum. The third concern stems from the instrumental profile of the HIRES and the

⁶<http://ssd.jpl.nasa.gov/cgi-bin/eph>

Hamilton spectrometers. It is known that the PSF is asymmetric to some degree (Valenti et al. 1995) and may give rise to systematic velocity shifts. However, it is unlikely that the same asymmetry in the same direction would be found at two different spectrometers. Therefore, we consider this possibility less plausible.

All Doppler measurements which used the NSO solar spectrum as the reference template were corrected for this offset of 522 m s^{-1} . Since currently no M dwarfs exist having a definitive barycentric radial velocity, the velocity zero-point for the M stars in our sample was set using the previously published velocities for the five standards from Marcy et al. (1987) which have errors of $\sim 0.4 \text{ km s}^{-1}$.

6. Comparison of Present Velocities with Standard Stars

To get an external measure of the accuracy of our barycentric radial velocities we have compared our velocities to published velocities of supposed radial velocity standard stars. We carry out this comparison separately for the FGK stars and for the M stars.

6.1. F, G and K Stars

We compared our velocities to those of the 26 standard stars that were measured by Udry et al. (1999a). The results of this comparison are shown in Figures 2 and 3 and yield $\langle V_{\text{Udry}} - V_{\text{Present}} \rangle = -53 \text{ m s}^{-1}$, with an rms scatter of 35 m s^{-1} . The corresponding uncertainty in the mean is $35/\sqrt{26} = 7 \text{ m s}^{-1}$. Thus the formal difference in zero points is

$$\langle V_{\text{Present}} - V_{\text{Udry}} \rangle = +53 \pm 7 \text{ m s}^{-1} \quad (1)$$

Thus, there appears to be a statistically significant difference in the zero-point of the velocities reported here compared to those of Udry et al. (1999a) of 53 m s^{-1} . We do not know the origin of this difference, nor do we know which scale is more “accurate”. Few studies will be affected by such small differences. But future highly precise proper motion measurements and precise orbit calculations may require such accurate velocities, including proper treatment of gravitational redshift and convective blueshift.

However, the difference between the present velocities and those of Udry et al. (1999a) do exhibit a significant $B-V$ dependence as seen in Figure 4. The slope of the linear trend is $-182 \pm 24 \text{ m s}^{-1}$ per mag with an RMS scatter around the fit of 23 m s^{-1} . This dependence

is similar to the $B-V$ dependence seen between the CfA and CORAVEL data (Stefanik et al. 1999; Udry et al. 1999a). This color dependence is likely caused by some spectral type mismatch in one or all of the radial-velocity scales. For solar type stars (near G2V) where our zero-point is well set, we are in good agreement with the CORAVEL velocities, with an offset of only 25 m s⁻¹ as seen in Figure 4.

According to Udry et al. (1999a) the ELODIE measurements ensure temporal stability of better than 15 m s⁻¹ during time scales of years for their standard stars. However, their quoted velocities have been rounded off at the 50 m s⁻¹ level. From our measurements of these stars in common, the temporal variability is less than 10 m s⁻¹ during \sim 5 yr. Therefore it is not certain whether the rms scatter of 35 m s⁻¹ between the two sets of velocities is due to our errors or the rounding of the ELODIE data plus their errors. We conclude that the barycentric velocities reside on the same scale with an offset of \sim 50 m s⁻¹, and a scatter of \sim 35 m s⁻¹.

Comparing our velocities for 29 common stars with those reported by Stefanik et al. (1999), with a correction of +136 m s⁻¹ added to their native velocities in Table 1 and 2 (Stefanik private communication), we obtain $\langle V_{\text{CfA}} - V_{\text{Present}} \rangle = 15$ m s⁻¹ which is only marginally different from zero, with an RMS scatter of 123 m s⁻¹ as seen in Figure 5. The differences exhibit a significant $B-V$ dependence as seen in Figure 6. The slope of the linear trend is $+448 \pm 111$ m s⁻¹ per mag with an RMS scatter around the fit of 109 m s⁻¹. This color dependence is likely caused by some spectral type mismatch in one or all of the radial-velocity scales. For solar type stars, we are in good agreement with the CfA velocities, with no offset as seen in Figure 6. This is likely due to the CfA velocity zero-point being set by observations of minor planets as was also done for the present velocities.

Interestingly, the sign of the slope in Figure 6 is opposite of that in Figure 4 between the CORAVEL and present velocities. Since synthetic spectra were used to derive both the CfA and ELODIE velocities, which were used as the reference system in Udry et al. (1999a), (Stefanik et al. 1999; Baranne et al. 1996; Gullberg 1999) this seems to give credence to the notion that using synthetic spectra does not entirely solve the problem of spectral dependent systematic errors.

6.2. M stars

The radial-velocity standard stars listed by Udry et al. (1999a) do not include any M dwarfs, and we do not have any M dwarfs in common with Stefanik et al. (1999) or the older CORAVEL standard stars (Udry et al. 1999b). Therefore, we compared our present

velocities for M dwarfs to those given in Marcy et al. (1987). The results of this comparison, for 21 stars in common, are shown in Figures 7 and 8 and yield $\langle V_{MLW} - V_{Present} \rangle = -21$ m s $^{-1}$ with an rms scatter of 164 m s $^{-1}$. The offset is obviously very low since the M star reference spectrum was created using the velocities quoted by Marcy et al. (1987). Since the average internal error for the velocities in Marcy et al. (1987) is ~ 200 m s $^{-1}$, most of the scatter in the differences is due to them. No $B-V$ dependence is seen in the residuals. It is therefore difficult to ascertain the uncertainty in our present velocities for M dwarfs and similarly difficult to ascertain a zero-point error (whatever that would mean). But a conservative estimate of the errors would be the ~ 0.4 km s $^{-1}$ uncertainty of the Marcy et al. (1987) velocities which were used in setting the velocity zero-point.

Since the observed offset (21 m s $^{-1}$) for the M dwarfs is within a factor of two of the internal scatter of ~ 10 m s $^{-1}$, we have not applied any correction to the radial velocities for these stars. There is some concern that our two sets of stars, the F, G, and K stars and the M stars, might not be on the same velocity zero-point. A comparison between them is difficult due to the significant spectral type mismatch errors.

7. Uncertainty Estimates

Due to the several systematic errors affecting radial velocities on the order of 0.1 km s $^{-1}$ it is difficult to ascertain the true uncertainties of the velocities reported here. Normally two different methods are used to estimate uncertainties: 1) Standard deviation of the mean (i.e. the internal RMS scatter of points), and 2) comparison with published values. We have done both here. On average the standard deviation of the mean, due to the internal scatter of points, for the velocities in Table 1 is ~ 10 m s $^{-1}$. We also compared our velocities with the best known published standard star velocities of Udry et al. (1999a). This comparison, as shown in the previous section, gave an RMS scatter of the differences of 35 m s $^{-1}$. Therefore, using the traditional methods of estimating uncertainties our velocities are accurate to ~ 35 m s $^{-1}$.

In this case the traditional methods fail due to the astrophysical sources of errors that affect all spectroscopic measurements of radial velocity. The values of these errors are not known adequately, otherwise we would have corrected for them. It is likely that these systematic errors were also not taken into account by Udry et al. (1999a) or Stefanik et al. (1999). This means that a comparison between their data and ours will not yield the true uncertainty of our velocities or theirs.

What the comparison does show is the precision of velocities within a given spectral

type. The velocities of all stars of a given spectral type will have a nearly constant offset from their true kinematic velocities, because the systematic errors are dependent on spectral type. Relative to that constant offset the velocities in that spectral type are very precise. The comparison with Udry et al. (1999a) shows our precision to be no worse than 0.035 km s^{-1} (see Fig. 3).

This high precision within a spectral type can be effectively used to look for moving groups. Moving groups have velocity dispersions of typically $\sim 0.5 \text{ km s}^{-1}$ such as the Pleiades group (Jones 1970). The present velocities are precise enough within a spectral type to judge whether a star belongs to the moving group or not.

Even though the exact values of the systematic errors are not known we can estimate our true uncertainties. There are three major systematic errors in our velocities, namely, convective blueshift, gravitational redshift and spectral type mismatch. These errors change systematically with spectral type. Since our velocity zero-point was set here using the day sky and the minor planet Vesta, which have well known radial velocities due to Solar System dynamics, the systematic errors were forced to zero for solar-type stars. The errors will rise as the spectral type departs from solar-type. Because the zero-point calibration was used for all FGK-type stars there will be differential errors due to convective blueshift and gravitational redshift that increase with departure from solar-type. Similarly, the spectral type mismatch errors only occur for non solar-type stars, since the NSO solar spectrum was used for the reference, and is therefore unaffected by the velocity zero-point calibration.

The approximate values of the systematic errors are as follows. According to Dravins (1999) the convective blueshift is approximately -1000 m s^{-1} for F5V ($B-V=0.4$), -400 m s^{-1} for G2V (solar-type, $B-V=0.64$), and -200 m s^{-1} for K0V ($B-V=0.9$). The effective velocity error caused by gravitational redshift can be computed from, $V_{\text{grav}} = GM/Rc$ (Dravins et al. 1999). We find, with masses and radii given by Allen (2000), that the redshift is $+680 \text{ m s}^{-1}$ for F5V, $+636 \text{ m s}^{-1}$ for G2V, and $+590 \text{ m s}^{-1}$ for K0V. The sum of the two effects shows that the overall systematic error is approximately -320 m s^{-1} for F5V, $+236 \text{ m s}^{-1}$ for G2V, and $+390 \text{ m s}^{-1}$ for K0V. Due to our zero-point calibration these errors are here forced to zero for solar-type stars. **Therefore, we expect that our velocities are low by $\sim 556 \text{ m s}^{-1}$ for F5V stars, true for solar-type stars, and high by $\sim 154 \text{ m s}^{-1}$ for K0V stars.**

With these estimates of the systematic errors in hand we can compute a correction for the velocities as a function of $B-V$. We fit a line to the first two points (F5V and G2V) and to the second two points (G2V and K0V) to obtain two linear interpolations. The first equation, Eqn (2), is for main-sequence stars earlier than solar-type ($B-V < 0.64$), and the second equation, Eqn (3), is for main-sequence stars later than solar-type ($B-V > 0.64$),

not including M type stars. Equation (3) may be used for stars with $1.3 > B-V > 0.9$, but represents an extrapolation of the points given above and should be used with caution. Since most of our main-sequence stars have $B-V < 1.1$ this shouldn't cause too many problems. These equations do not account for spectral type mismatch errors because we do not know enough about these effects yet for our velocities.

$$RV_{\text{kin}} = RV_{\text{spec}} - 2.317 \times (B-V) + 1.483 \text{ km s}^{-1} \quad B-V < 0.64 \quad (2)$$

$$RV_{\text{kin}} = RV_{\text{spec}} - 0.642 \times (B-V) + 0.411 \text{ km s}^{-1} \quad 0.64 < B-V < 1.3 \quad (3)$$

These corrections are valid only for main-sequence stars for which the NSO solar spectrum was used as the reference. The velocities for the M type stars, with $B-V > 1.3$ and for which the M composite spectrum was used as the reference, have a zero-point uncertainty of $\sim 0.4 \text{ km s}^{-1}$ and therefore a correction for gravitational redshift or convective blueshift is not warranted at this time. However, we expect the velocities of the M stars to be very precise due to their low RMS velocity scatter and their small spectral type range which minimizes the systematic errors. We expect them to also be precise to 0.03 km s^{-1} , just as the FGK main-sequence stars. If the “true” radial velocity of only one of them were known then they all could be corrected for their zero-point error and be very accurate.

We expect that the corrections given in equations (2) and (3) account for convective blueshift and gravitational redshift to within $\sim 0.1 \text{ km s}^{-1}$. The errors due to spectral type mismatch are likely to be $\sim 0.1 \text{ km s}^{-1}$ (Griffin et al. 2000). From the errors expressed in equations (2) and (3), an additional $\sim 0.1 \text{ km s}^{-1}$ for the spectral type mismatch error, along with the distribution of spectral types of our survey stars, the typical uncertainty of the uncorrected radial velocities in Tables 1 and 2 is $\sim 0.3 \text{ km s}^{-1}$. For the few subgiants, the errors are somewhat larger, but not easily estimated without models of subphotospheric convection in such stars.

We cannot at this time give a correction for the velocities of our 45 giants. Giants have a gravitational redshift on the order of 0.1 km s^{-1} which is much smaller than that for dwarfs due to the large radius of giants, $\sim 15 R_\odot$ (Allen 2000). The convective blueshift is not known for giants and hinders us from giving a rough velocity correction. Hopefully, more in-depth future studies of the sources of error discussed here, such as recent work by Pourbaix et al. (2002), will allow for more accurate corrections of radial velocities and eventually yield “true” radial velocities. Until that time these corrections may be used for the present velocities.

8. Final Radial Velocities and Description of Tables

The barycentric radial velocities for all 889 stars are reported in Tables 1 and 2. The 782 stars that exhibit an RMS velocity scatter less than 100 m s^{-1} are reported in Table 1. Primary and alternate star names are given in the first two columns, and the stellar spectrum used as the template (either NSO or M dwarf composite) is listed in column three. The mean time of the observations is given in column four under $\langle \text{JD} \rangle$ to establish the characteristic epoch for the velocity measurement. The span of observations in days is given in column five, and the mean barycentric radial velocity of all observations for a star is in column six. Stars with only one observation were put in Table 1 even though their RMS scatter is not defined. They can be distinguished by $\Delta T = 0$.

The 107 stars with an RMS velocity scatter greater than 100 m s^{-1} are reported in Table 2. Primary and alternate star names are given in the first two columns. The stellar template spectrum (either NSO or M dwarf) is given in column three. The Julian Date (JD) of one specific observation is given in column four. The barycentric radial velocity of that one observation is given in column five. The mean date of all observations and span of observations are given in columns six and seven. The RMS scatter of the velocities of all observations is given in column eight, and the number of observations in column nine. The last column is for comments where stars with companion orbits or linear trends are noted. “L” indicates that velocities vary linearly with time (see Table 4), “CO” indicates that a companion and its orbit were found, “C” indicates that a published companion exists but an orbit is not given here, and ”A” indicates that the star is chromospherically active based on the emission reversal seen at the CaII H&K lines in our spectra.

The orbital parameters for 15 stars with companions are reported in Table 3. The orbital period P , velocity semi-amplitude K , eccentricity e , longitude of periastron ω , and time of periastron T_0 are given as well as the primary mass M_1 , minimum secondary mass $M_{2,\min}$, minimum semi-major axis a_{\min} , and the mass function, $f(M)$. References are also given to other sources which have information on these stars, their companions and orbital parameters. The data for stars with linear trends are given in Table 4. The slope of the radial velocity curve and the number of observations is given for 30 stars.

9. Orbits of Binaries

We found 107 stars in this program that exhibit an RMS velocity scatter greater than 100 m s^{-1} . We attempted to fit these with a Keplerian orbit. We found 29 stars that yield good Keplerian orbital fits to their relative radial velocities. Many of these binaries have been

previously published from our velocities and therefore will not be duplicated here. Several papers contain these previously reported single-line spectroscopic binaries, namely Marcy et al. (1999), Butler et al. (2000), Vogt et al. (2002), Fischer et al. (2002), Cumming et al. (1999), Marcy et al. (2001b).

For 15 stars, our velocities provide unpublished orbital solutions or reveal unknown companions. These orbits are listed in Table 3 which gives the usual orbital parameters for single-line spectroscopic binaries. Plots of the velocities and the associated Keplerian fits are shown in Figures 9–23. The mass for the primary star for each system was estimated from the catalog by Prieto & Lambert (1999) or by using $B-V$ and Allen (2000). From the orbital parameters and primary masses, we determined the minimum companion masses (M_{\min}), mass functions, $f(M)$, and minimum semimajor axes, a_{\min} , which are also listed in Table 3. The values of M_{\min} range from $42 M_{\text{Jup}}$ to $545 M_{\text{Jup}}$, and therefore the companions are all candidate brown dwarfs or H-burning stellar companions. The uncertainties in the orbital parameters were found by a Monte Carlo technique in which Gaussian velocity noise was added to the best-fit theoretical velocity curve at the times of observation. We ran 50 trials for each case, with orbital parameters being rederived for each trial. The standard deviations of the resulting orbital parameters were taken as the uncertainties. For some stars the Monte Carlo method underestimated the uncertainties in the orbital parameters. For these stars a more conservative estimate of the uncertainties was made by fitting many different Keplerian orbits to the observed relative radial velocities, without any modeled Gaussian noise, and then looking at the scatter of the parameters produced by the best orbital fits.

The stars HD4747, HD65430 and GJ84 have large orbital uncertainties due to incomplete phase coverage. There were insufficient velocity measurements to constrain the orbit of HD18445 even though it is known to have a companion (Halbwachs et. al 2000). Thus it isn't listed in Table 3. The eccentricity for HD140913 was fixed to $e = 0.54$ (Latham et al. 1989) in performing the Keplerian fit, since not enough points were available to constrain the eccentricity. Only the other four parameters were fit for this star. The Keplerian fit for HD208776 is particularly poor as insufficient velocities are available to constrain the orbital period to better than a factor of two. Eleven of the spectroscopic binary stars appear to be newly discovered here: HD4747, HD7483, HD30339, HD34101, HD39587, HD65430, HD174457, HD208776, GJ84, GJ595, HIP52940. Velocities are available upon request of G.M. The companions all have M_{\min} in the sub-stellar range or low mass stellar range, and thus offer interesting targets for studies with adaptive optics or interferometry.

10. Conclusion

We have provided barycentric radial velocities with an internal precision of 0.03 km s^{-1} for 889 stars. The error estimates stem both from the internal errors found from the spectral chunks within each spectrum and from the comparison with accurate velocities on the CORAVEL scale (Udry et al. 1999a). The radial velocities of the F, G and K dwarfs reside on a velocity zero-point defined by the observations of the Sun, using the day sky and Vesta as proxies. Our velocity scale differs by only 0.053 km s^{-1} from that of Udry et al. (1999a) and 0.015 km s^{-1} from that of Stefanik et al. (1999), thus adding confidence to the zero points of all three sets of velocities. The radial velocities of the M dwarfs reside on the velocity system defined by Marcy et al. (1987) and have not been further corrected, nor is such a correction known to be necessary. These M dwarf velocities are probably accurate to within 200 m s^{-1} .

The Doppler shifts reported here have such high accuracy that gravitational redshift and convective blueshift impose comparable (or greater) wavelength shifts. These effects were somewhat removed from our velocity measurements by using the Sun for the velocity zero-point. We expect therefore that for G2V stars the present velocities represent their “true” kinematic velocities within 0.03 km s^{-1} . However, for stars departing from solar-type the sum of the two astrophysical effects will produce systematic errors dependent on spectral type. From F to K type dwarfs this variation will be as large as $\sim 0.3 \text{ km s}^{-1}$ and will cause our velocities to be low for F type stars and high for K type stars. Using estimates for these effects we give rough velocity corrections in equations (2) and (3). We presume that these corrections bring the velocities within $\sim 0.15 \text{ km s}^{-1}$ of their “true” kinematic values.

These precise radial velocities can be used to complement future highly precise proper motion measurement, such as those projected to be obtained by the GAIA mission of the ESA. The radial velocities and proper motions will give the three components of space motion of stars. These precise space motions may be useful for discerning the membership of moving groups, since young moving groups have velocity dispersions of $\sim 0.5 \text{ km s}^{-1}$ (Jones 1970).

The 782 stars listed in Table 1 exhibited a velocity scatter of less than 100 m s^{-1} during 4 years. These stars apparently exhibit relatively stable velocities on time scales of a decade and represent candidates for radial velocity standard stars. However, their integrity as velocity standard stars requires future observations to verify their stability. We expect that some of these 782 “stable” stars may reveal slow drifts in radial velocity on time scales longer than 10 yr.

The accuracy of the present velocities offers an opportunity to detect such slow drifts by future measurements made with comparable accuracy. Such velocity variations may prove

useful in identifying unseen companions at large orbital distances, i.e., over 10 AU. We found that 107 stars exhibited velocity variations of over 100 m s⁻¹ (RMS). For these stars, we have provided the RMS velocity, and also either an orbital solution or a description of the linear trends. We intend these measurements to provide dynamical constraints on the nature of the companions.

We acknowledge support by NSF grant AST-9988358 (to SSV), NSF grant AST-9988087 and travel support from the Carnegie Institution of Washington (to RPB), NASA grant NAG5-8299 and NSF grant AST95-20443 (to GWM), and by Sun Microsystems. We thank the NASA and UC Telescope assignment committees for allocations of Keck telescope time, and we thank the University of California for generous allocations of telescope time at Lick Observatory. This research has made use of the Simbad database, operated at CDS, Strasbourg, France. We would like to thank A. Reines, C. McCarthy, E.J. Anderson, and S. White for all of their help and inspiration.

REFERENCES

- Allen, C. W. 2000, Astrophysical Quantities, Fourth Edition, AIP Press.
- Allende Prieto, C., García López, R. J. & Trujillo Bueno, J., 1997, ApJ, 483, 941
- Baranne, A. 2000, IAU Coll 170, 41
- Baranne, A., Queloz, D., Mayor, M., Adrianzyk, G., Knispel, G., Kohler, D., Lacroix, D., Meunier, J.-P., Rimbaud, G., & Vin, A. 1996, Astronomy & Astrophysics Supplement, 119, 337
- Barbieri, C., Demarchi, G., Nota, A., Corrain, G., Hack, W., Ragazzoni, R., & Macchietto, D. 1996, A&A, 315, 418
- Beavers, W. I., & Salzer, J. J. 1983, PASP, 95, 79
- Binney, J. & Merrifield, M. 1998, in Galactic Astronomy, Princeton Univ. Press, g1 pg 38.
- Blazit, A., Bonneau, D., & Foy, R. 1987, A&AS, 71, 57
- Bouchy, F., Pepe, F., Queloz, D. 2001, A&A, 374, 733
- Butler, R. P., Marcy, G. W., Williams, E., McCarthy, C., Dosanjh, P., & Vogt, S. S. 1996, PASP, 108, 500
- Butler, R. P., Marcy, G. W., Williams, E., Hauser, H., & Shirts, P. 1997, ApJ, 474, L115
- Butler, R. P., Vogt, S. S., Marcy, G. W., Fischer, D. A., Henry, G. W., & Apps, K. 2000, ApJ, 545, 504
- Carroll, B. W., & Ostlie, D. A. 1996 An Introduction to Modern Astrophysics, Addison-Wesley Publishing Co., A-14
- Cumming, A. et al. 1998, ApJ.
- Dravins, D., Gullberg, D., Lindegren, L., & Madsen, S. 1999, IAU Coll 170, 41
- Dravins, D. 1999, IAU Coll 170, 268
- Duquennoy, A., & Mayor, M. 1991, A&A, 248, 485
- Fischer, D. A. et al. 2002, in preparation
- Gray, D. F. The Observation and Analysis of Stellar Photospheres, Cambridge University Press.

- Gray, D. F. 1999, IAU Coll 170, 243
- Griffin, R. E. M., David, M., & Verschueren, W. 2000, A&AS, 147, 299
- Gullberg, D. 1999, IAU Coll 170, 58
- Halbwachs, J. L., Arenou, F., Mayor M., Udry, S., & Queloz D. 2000, A&A, 355, 581
- Henry, T. J., & McCarthy, D. W., Jr. 1993, AJ, 106, 773
- Jones, Burton F. 1970, AJ, 75, 563
- Kamper, K. W. 1987, AJ, 93, 683
- Kamper, K. W., & Lyons, R. W. 1981, JRASC, 75, 56
- Kurucz, R. L., Furenlid, I. & Brault, J., 1984, Flux Atlas from 296 to 1300 nm, Sunspot, NM: National Solar Observatory
- Latham, D. W., Mazeh T., Stefanik, R. P., Mayor M., & Burki G. 1989, Nature, 339, 38
- Lindgren, L., Dravins, D., & Madsen, S. 1999, IAU Coll 170, 73
- Lippincott, S. L., & Worth, M. D. 1978, PASP, 90, 330
- Marcy, G. W., & Butler, R. P. 1992, PASP, 104, 270
- Marcy, G. W., Butler, R. P., Fischer, D., Vogt, S. S., Lissauer, J. J., & Rivera, E. J. 2001b, ApJ, 556, 296
- Marcy, G. W., Butler, R. P., Vogt, S. S., Fischer, D., & Liu, M. C. 1999, ApJ, 520, 239
- Marcy, G. W., Butler, R. P., Vogt, S. S., Liu, M. C., Laughlin, G., Apps, K., Graham, J. R., Lloyd, J., Luhman, K. L., & Jayawardhana, R. 2001a, ApJ, 555, 418
- Marcy, G. W., Cochran, W. D., & Mayor, M. 2000, in Protostars and Planets IV, ed. V. Mannings, A. P. Boss & S. S. Russell (Tucson: University of Arizona Press), p1285.
- Marcy, G. W., Lindsay, V. & Wilson, K. 1987, PASP, 99, 490
- Marcy, G. W., & Moore, D. 1989, ApJ, 341, 961
- Martin, C., Mignard, F., Hartkopf, W. I., & McAlister, H. A. 1998, A&AS, 133, 149
- Mayor, M., Queloz, D., Udry, S., & Halbwachs, J. L. 1997, IAU Coll 161, 313

- Mazeh, T., Latham, D. W., & Stefanik, R. P. 1996, ApJ, 466, 415
- McCarthy, C. 1995, Master's Thesis, San Francisco State University
- McCarthy, D. W., Jr. 1986 in *Astrophysics of Brown Dwarfs*, ed. M. C. Kafatos, R. S. Harrington, and S. P. Maran (Cambridge: Cambridge University Press), p.9.
- McCarthy, D. W., Jr., & Henry, T. J. 1987, ApJ, 319, L93
- Misner, C. W., Thorne, K. S., & Wheeler, J. A. 1973, Gravitation, W. H. Freeman, San Francisco
- Oetiker, B., Duric, N., McGraw, J. T., & McGrath, M. A. 2001, PASP, 113, 703
- Pepe, F., Mayor, M., Delabre, B., Kohler, D., Lacroix, D., Queloz, D., Udry, S., Benz, W., Bertaux, J-L., Sivan, J-P., 2000, SPIE, 4008, 582
- Perryman et al. 1996, A&A, 310, L21
- Pourbaix,D., Nidever,D., McCarthy,C., Butler, R.P., Tinney,C.G., Marcy,G.W., Jones,H.R.A., Penny,A.J., Carter,B.D., Bouchy,F., Pepe,F., Hearnshaw,J.B., Skuljan,J., Ramm,D., Kent,D. 2002, submitted to AA.
- Prieto, C. A., & Lambert, D. L. 1999, A&A, 352, 555
- Saar, S. H. & Fischer, D. 2000, ApJ, 134, L105
- Skuljan, J., Hearnshaw, J. B., & Cottrell, P. L. 1999, IAU Coll 170, 91
- Stefanik, R. P., Latham, D. W., & Torres, G. 1999, IAU Coll 170, 354
- Udry, S., Mayor, M., & Queloz, D. 1999a, IAU Coll 170, 367
- Udry, S., et al. 1999b, IAU Coll 170, 383
- Udry, S., Mayor, M., & Queloz, D. 2000,
Planetary Systems in the Universe: Observations, Formation and Evolution, IAU Symp 202
- Valenti, J. A., Butler, R. P., & Marcy, G. W. 1995, PASP, 107, 966
- Vogt, S. S. 1987, PASP, 99, 1214.
- Vogt, S. S. et al. 1994, Proc. Soc. Photo-Opt. Instr. Eng., 2198, 362.

- Vogt, S. S., Marcy, G. W., Butler, R. P., & Apps, K. 2000, ApJ, 536, 902
- Vogt, S. S., Butler, R. P., Marcy, G. W., Fischer, D. A., Pourbaix, D., Apps, K., & Laughlin, G. 2002, submitted to ApJ
- Wagman, N. E. 1949, AJ, 54, 138

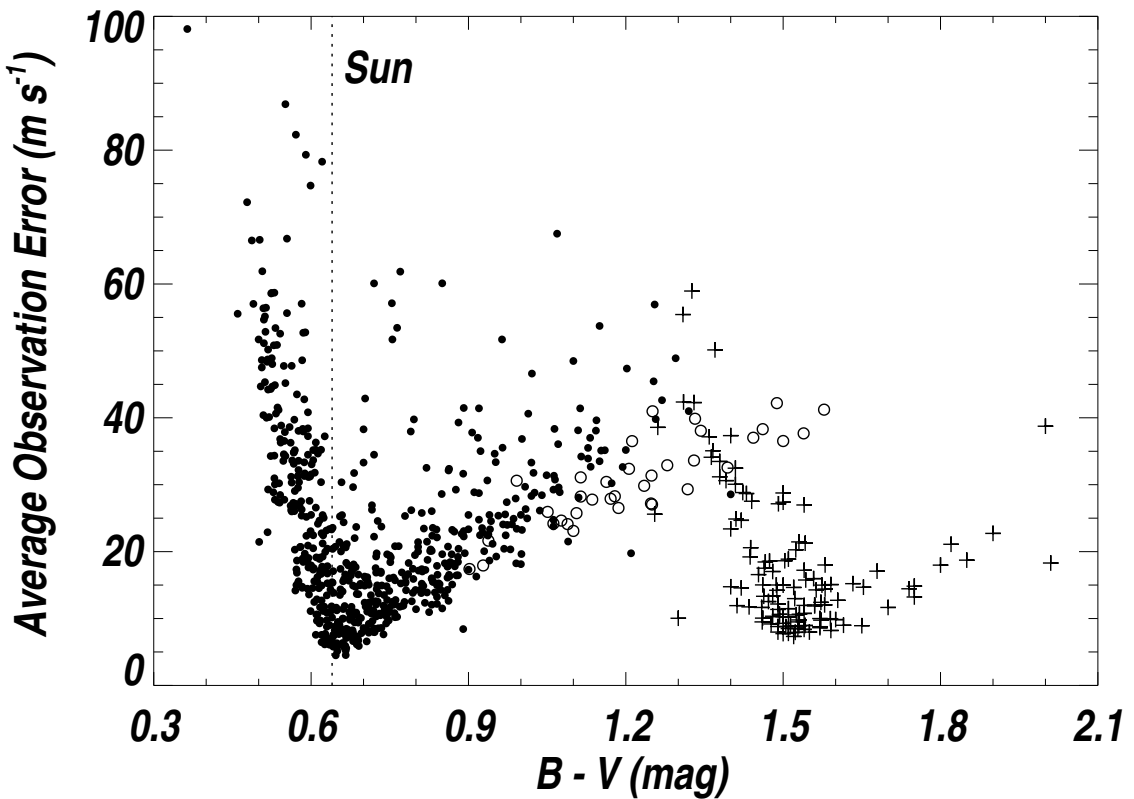


Fig. 1.— The internal velocity error per observation (averaged per star) vs. $B - V$. The dots represent the stars for which the NSO solar spectrum was used as the reference (filled dots represent dwarfs and open dots represent giants) and the plusses represent the stars for which the M star composite spectrum was used as the reference. The $B - V$ for the Sun ($B - V = 0.64$) is shown for clarity. The spectral type dependence of errors is apparent.

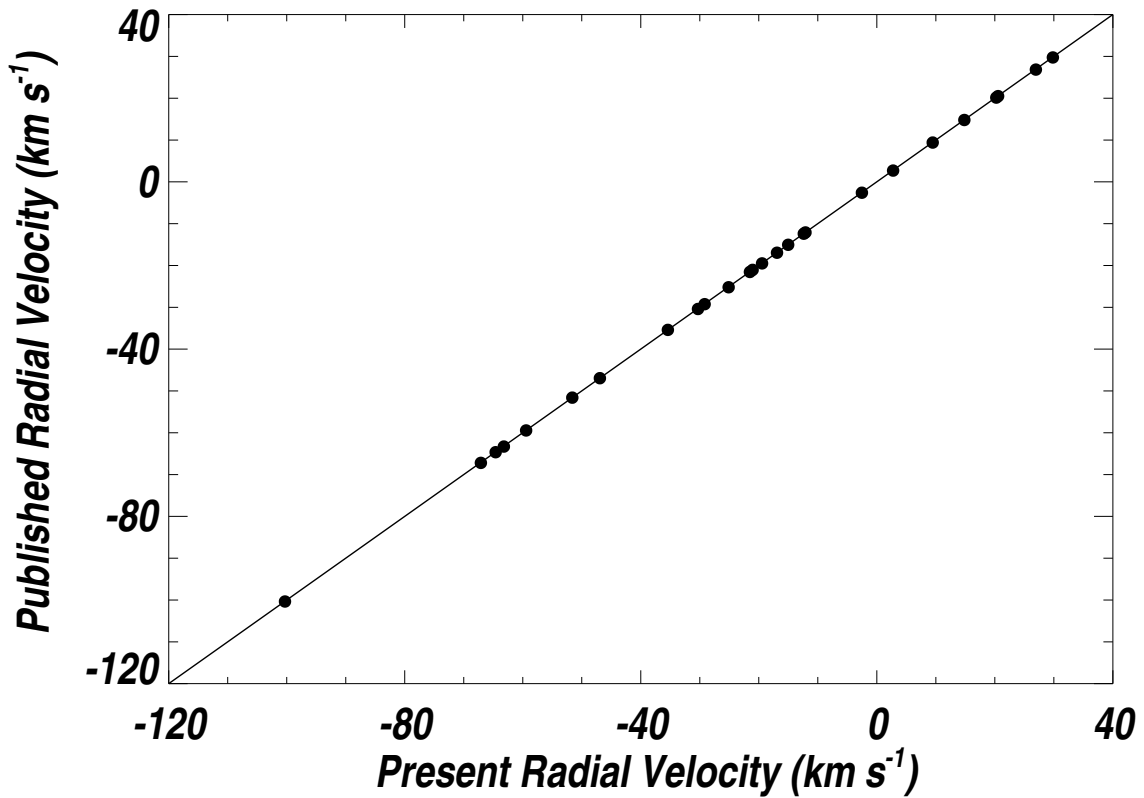


Fig. 2.— Velocities of standard stars vs. velocities measured here, for F, G, and K stars. The standard stars are on the CORAVEL scale (Udry et al. 1999a). The present velocities agree well with the standards, with no visible nonlinear departure of velocity scale.

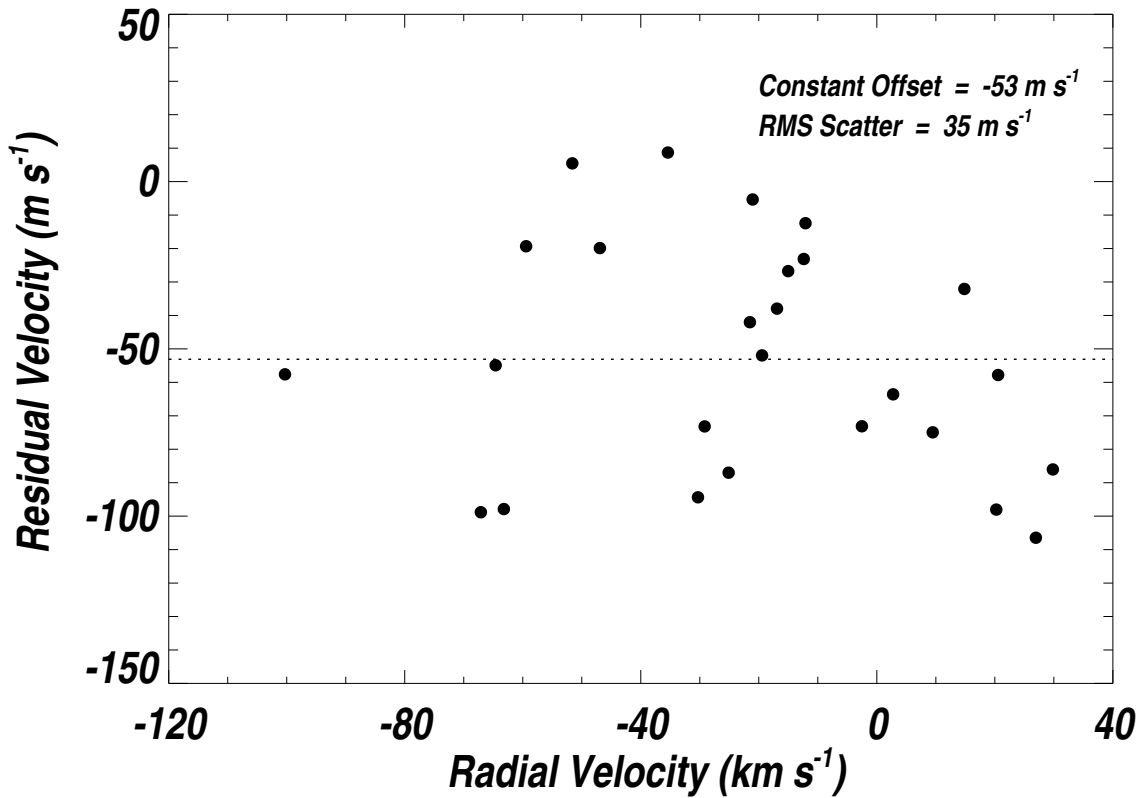


Fig. 3.— Standard-star velocities (Udry et al. 1999a) minus present velocities for all 26 FGK stars in common (as in Figure 2). The differences reveal that the present velocities are higher than those of Udry et al. by 53 m s^{-1} , and exhibit an rms scatter of 35 m s^{-1} . Thus the present velocities and those of Udry et al. (1999a) each have internal accuracy better than 35 m s^{-1} , and differ in zero-point by $\sim 53 \text{ m s}^{-1}$.

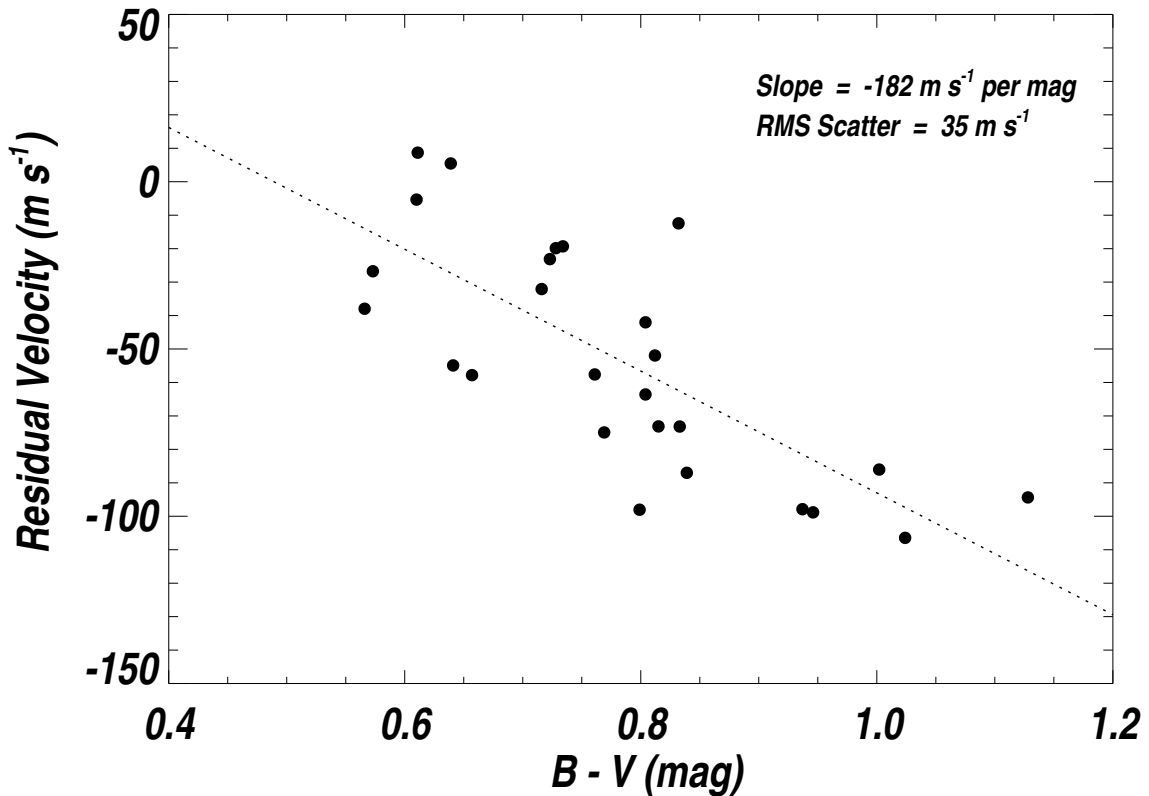


Fig. 4.— Standard-star velocities (Udry et al. 1999a) minus the present velocities as a function of $B - V$. A dependence is apparent, suggesting systematic errors in at least one set of velocities. The slope is $-182 \pm 24\ m\ s^{-1}$ per mag. The RMS scatter is $35\ m\ s^{-1}$ before fitting and $23\ m\ s^{-1}$ after fitting a line to the data.

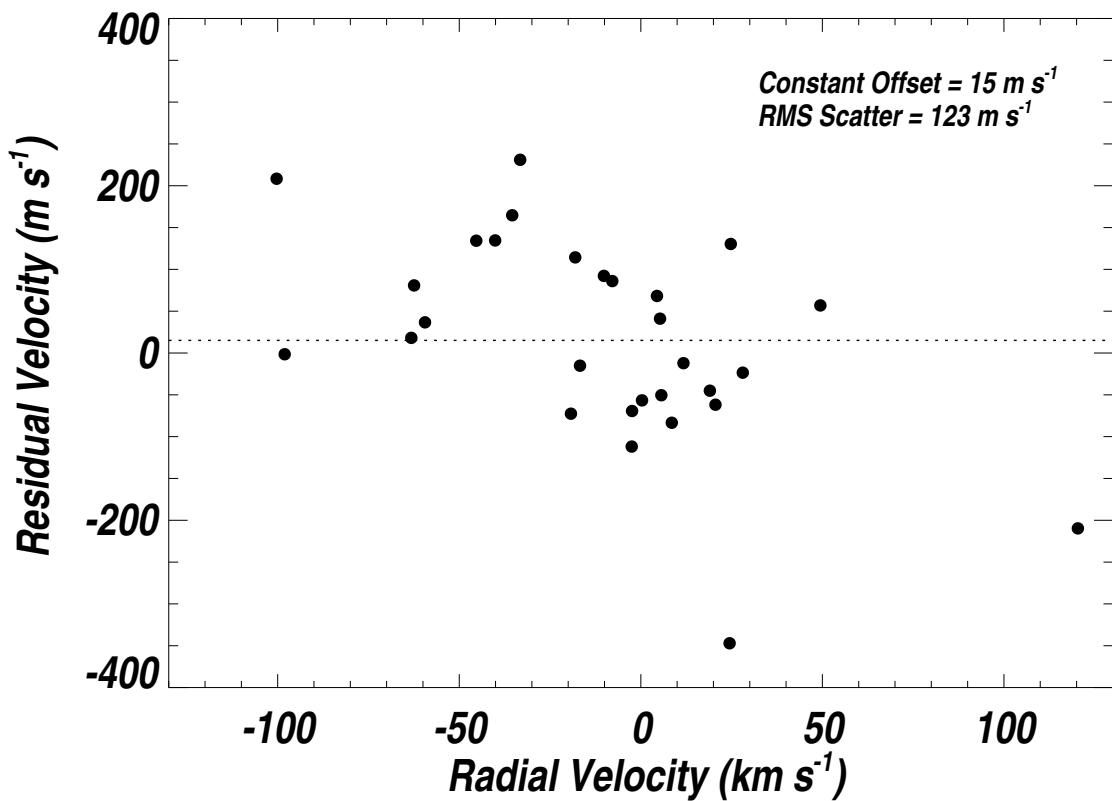


Fig. 5.— Standard-star velocities (Stefanik et al. 1999) minus present velocities for all 29 FGK stars in common. The differences reveal that the present velocities are lower than those of Stefanik et al. by $15\ m\ s^{-1}$, and exhibit an rms scatter of $123\ m\ s^{-1}$. Thus the present velocities and those of Stefanik et al. (1999) differ in zero-point by $\sim 15\ m\ s^{-1}$.

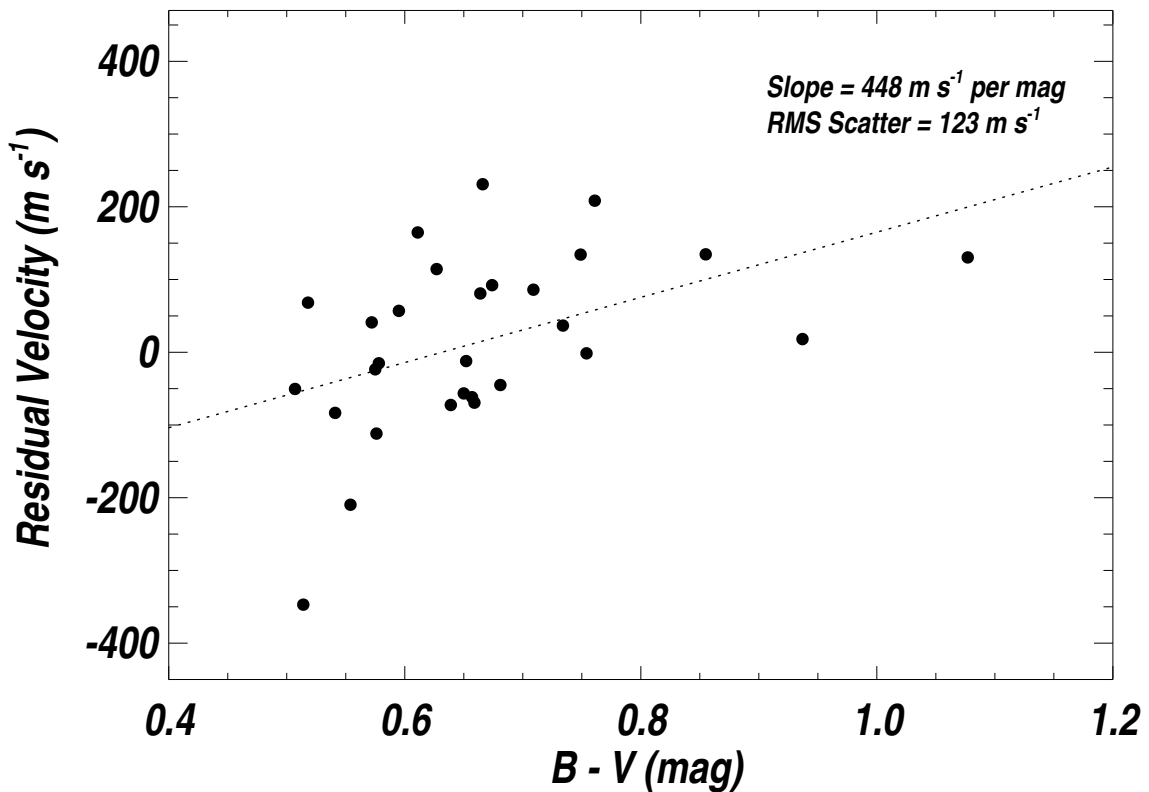


Fig. 6.— Standard-star velocities (Stefanik et al. 1999) minus the present velocities as a function of $B - V$. A dependence is apparent, suggesting systematic errors in at least one set of velocities. The slope is $+448 \pm 111\ m\ s^{-1}$ per mag. The RMS scatter is $123\ m\ s^{-1}$ before fitting and $109\ m\ s^{-1}$ after fitting a line to the data.

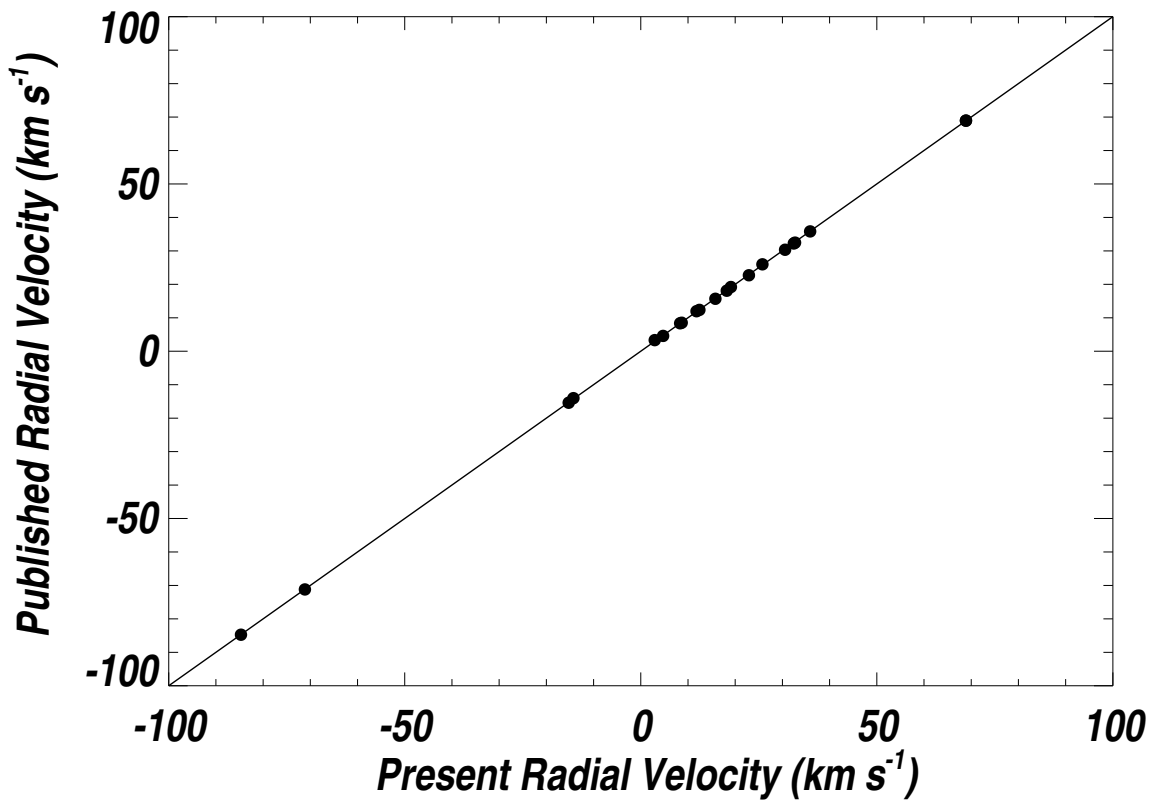


Fig. 7.— Velocities of standard stars (Marcy et al. 1987) vs. present velocities for M dwarfs. The velocities agree well with no apparent nonlinear dependence.

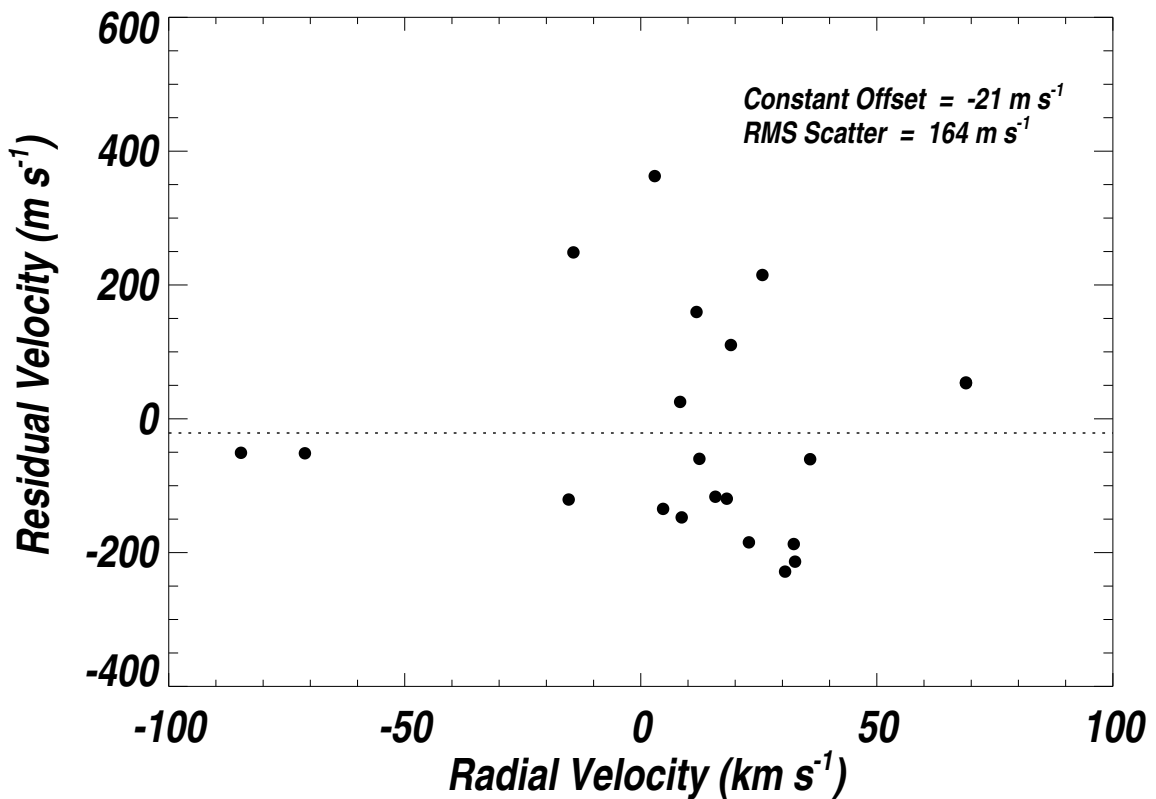


Fig. 8.— Difference between standard stars velocities (Marcy et al. 1987) and present velocities for all 21 M stars in common (as in Figure 7). There is an rms scatter of 164 m s^{-1} , and a constant offset of -21 m s^{-1} which is not statistically significant. Thus our velocities for the stars having $B-V > 1.3$ reside on the velocity scale set by Marcy et al. (1987). No $B-V$ dependence is seen in the residuals.

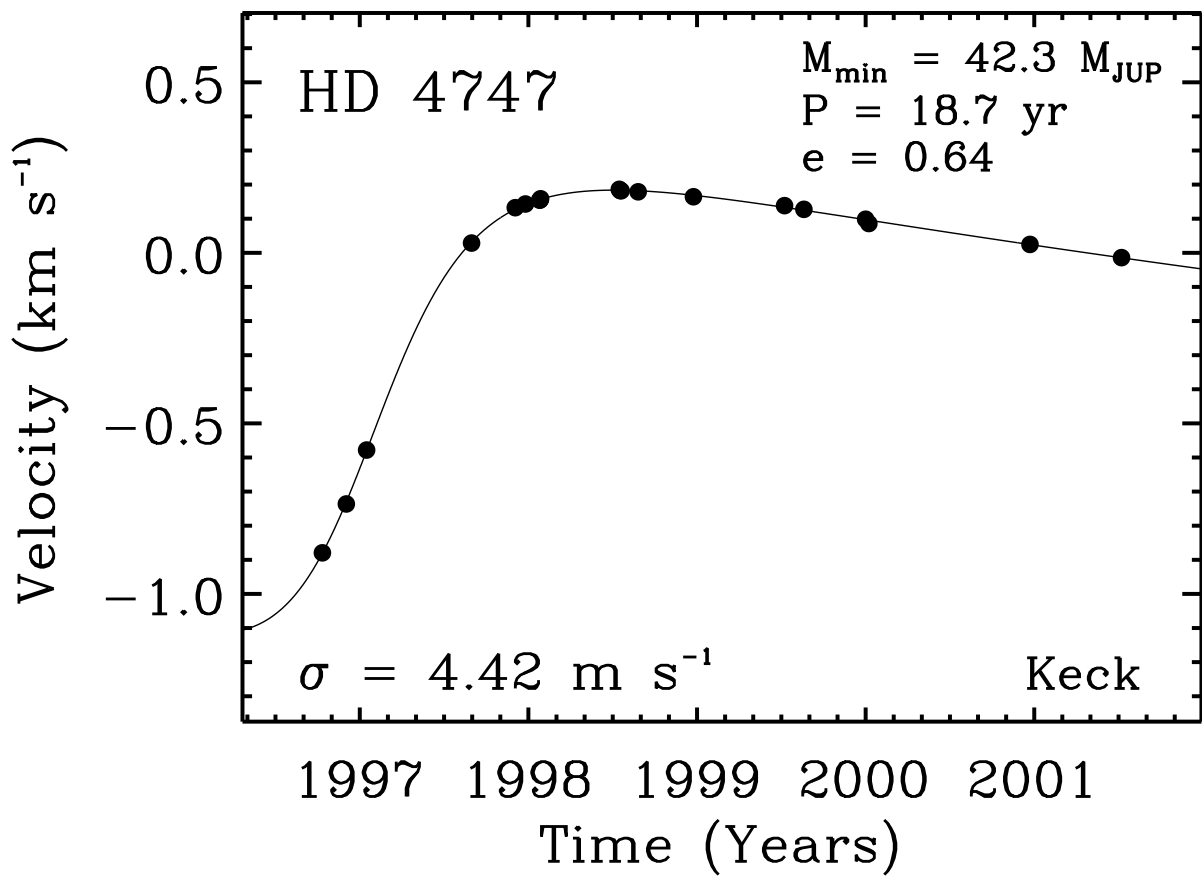


Fig. 9.— Doppler velocities for HD 4747 (G8/K0 V). The solid line is a Keplerian orbital fit with a period of 18.7 yr, a semiamplitude of 0.65 km s⁻¹, and an eccentricity of 0.64, yielding a minimum (M_{\min}) of 42.3 M_{JUP} for the companion. The RMS of the Keplerian fit is 4.42 m s⁻¹.

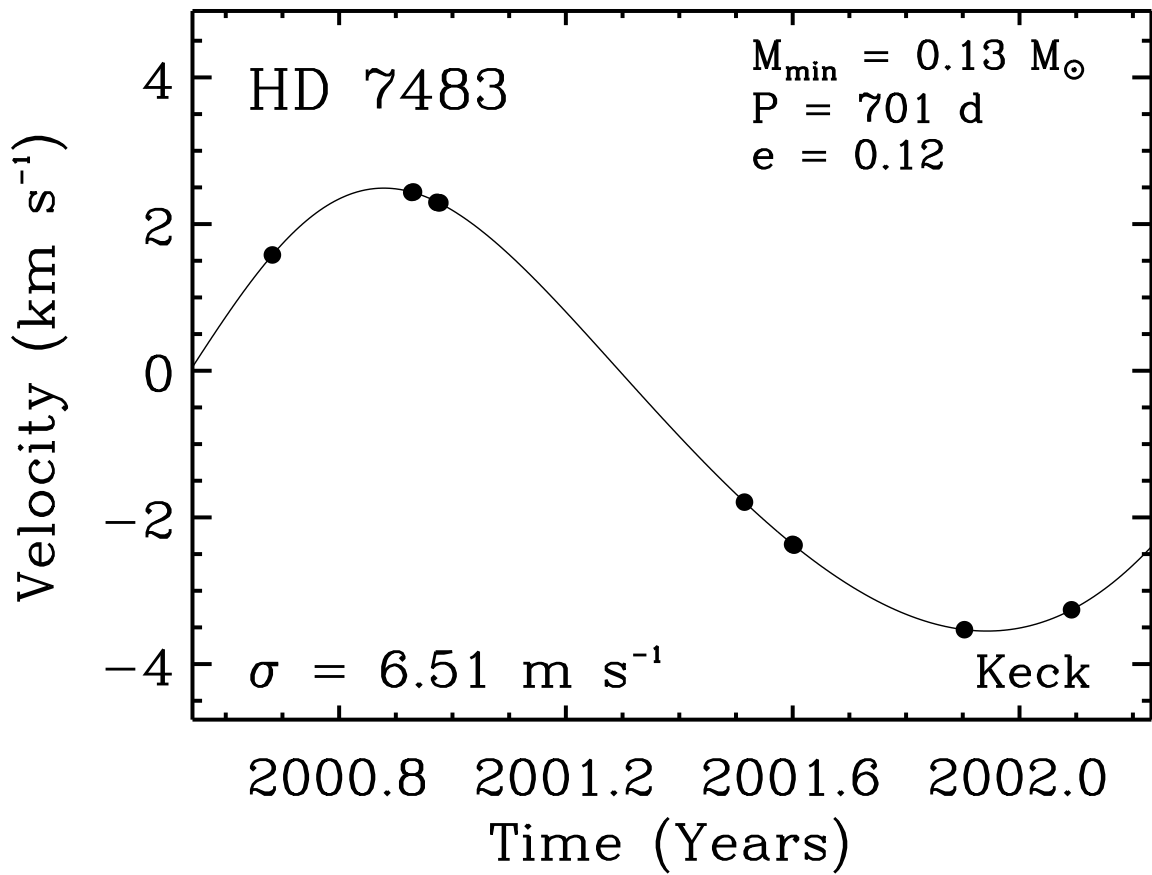


Fig. 10.— Doppler velocities for HD 7483 (G5 V). The solid line is a Keplerian orbital fit with a period of 701 d, a semiamplitude of 3.02 km s^{-1} , and an eccentricity of 0.12, yielding a minimum (M_{\min}) of $0.13 M_{\odot}$ for the companion. The RMS of the Keplerian fit is 6.51 m s^{-1} .

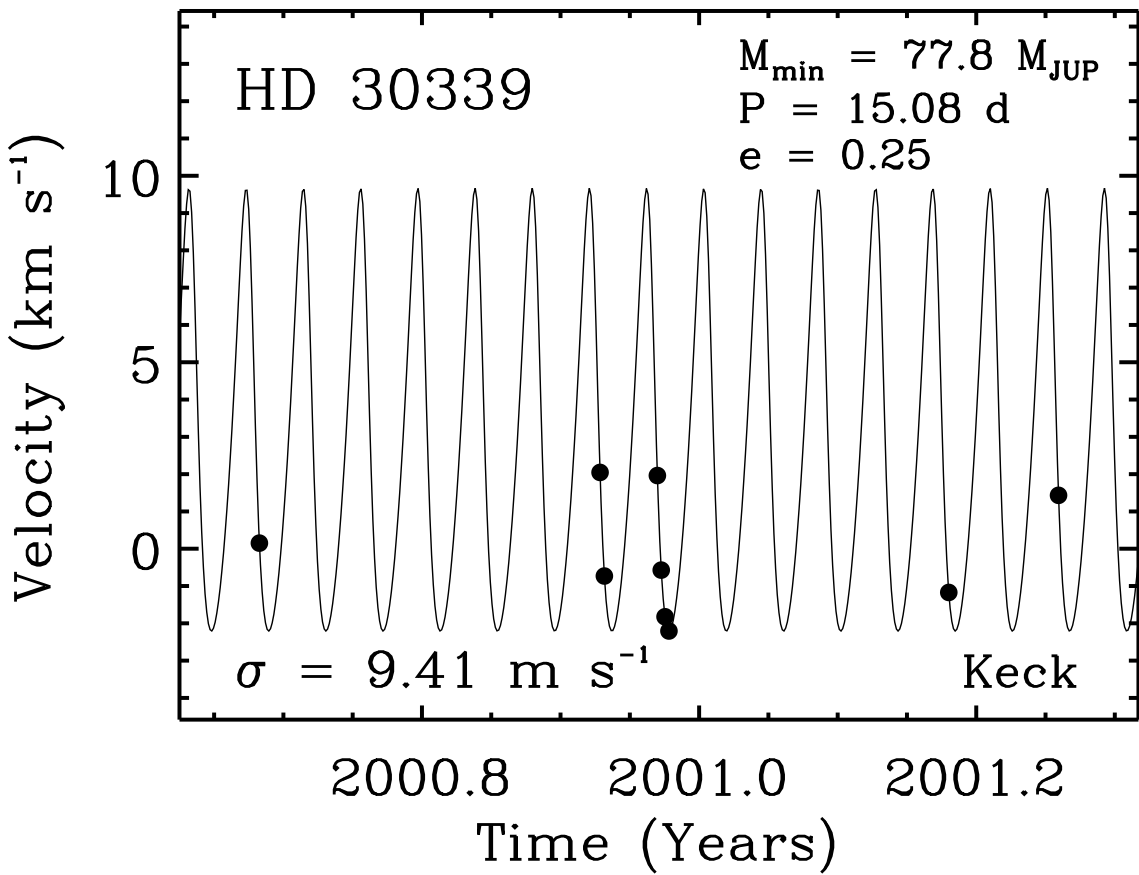


Fig. 11.— Doppler velocities for HD 30339 (F8 V). The solid line is a Keplerian orbital fit with a period of 15.08 d, a semiamplitude of 5.94 km s⁻¹, and an eccentricity of 0.25, yielding a minimum (M_{\min}) of 77.8 M_{JUP} for the companion. The RMS of the Keplerian fit is 9.41 m s⁻¹.

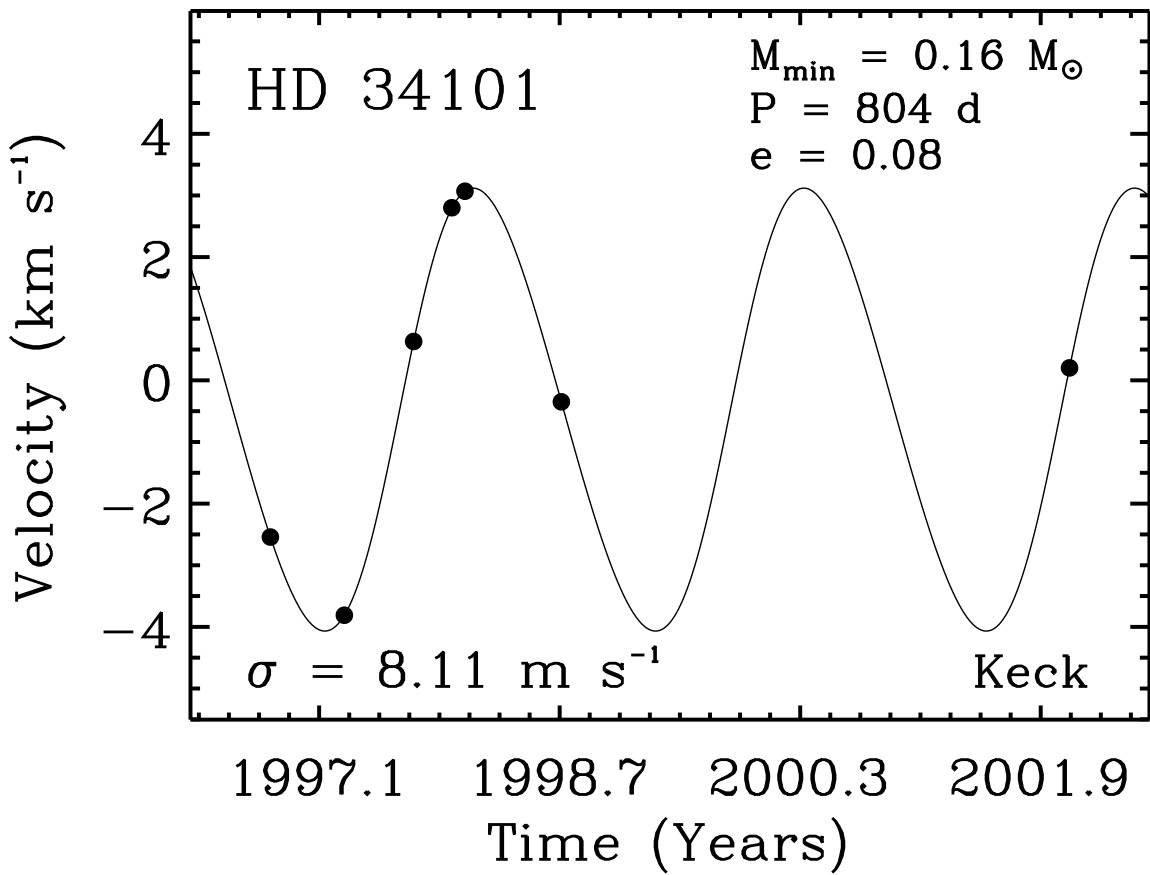


Fig. 12.— Doppler velocities for HD 34101 (G8 V). The solid line is a Keplerian orbital fit with a period of 804 d, a semiamplitude of 3.76 km s^{-1} , and an eccentricity of 0.08, yielding a minimum (M_{\min}) of $0.16 M_{\odot}$ for the companion. The RMS of the Keplerian fit is 8.11 m s^{-1} .

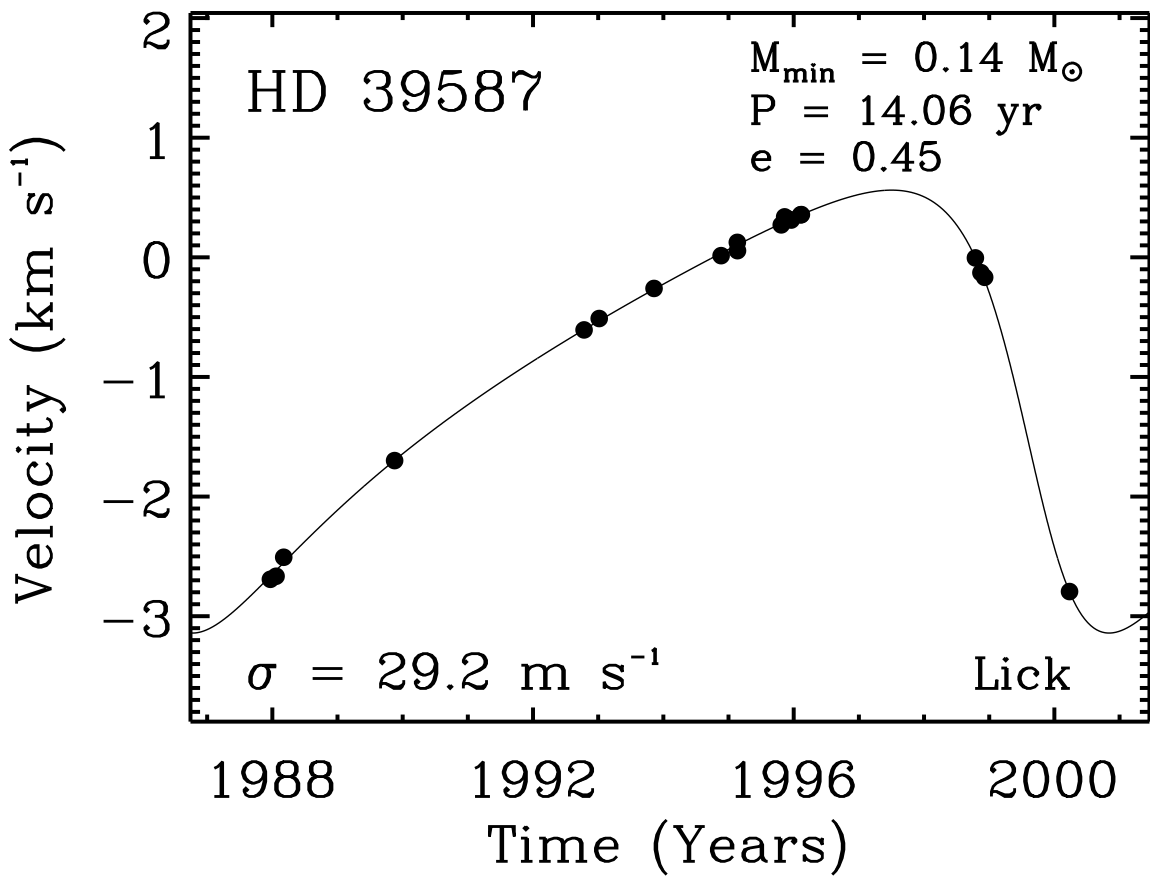


Fig. 13.— Doppler velocities for HD 39587 (G0 V). The solid line is a Keplerian orbital fit with a period of 14.06 yr, a semiamplitude of 1.85 km s⁻¹, and an eccentricity of 0.45, yielding a minimum (M_{\min}) of $0.14 M_{\odot}$ for the companion. The RMS of the Keplerian fit is 29.2 m s⁻¹.

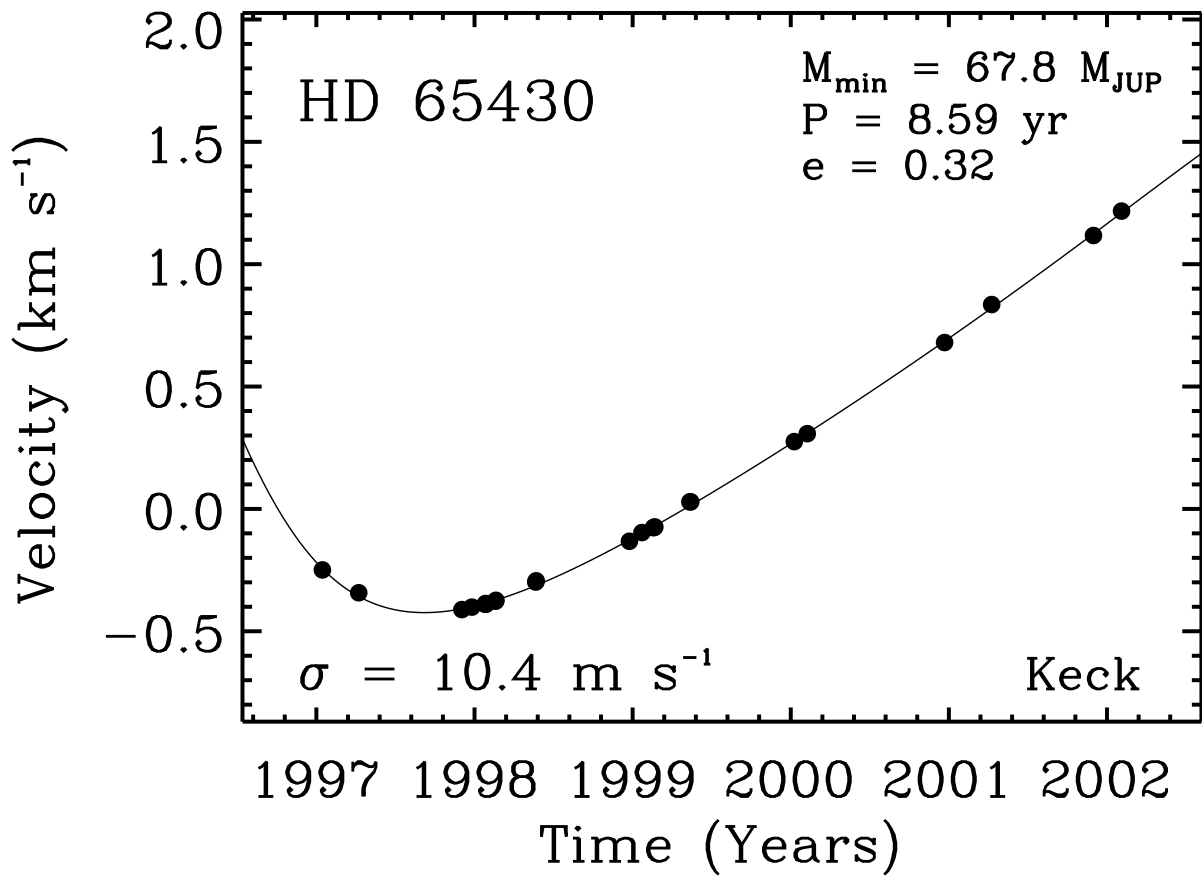


Fig. 14.— Doppler velocities for HD 65430 (K0 V). The solid line is a Keplerian orbital fit with a period of 8.59 yr, a semiamplitude of 1.11 km s⁻¹, and an eccentricity of 0.32, yielding a minimum (M_{\min}) of 67.8 M_{JUP} for the companion. The RMS of the Keplerian fit is 10.4 m s⁻¹.

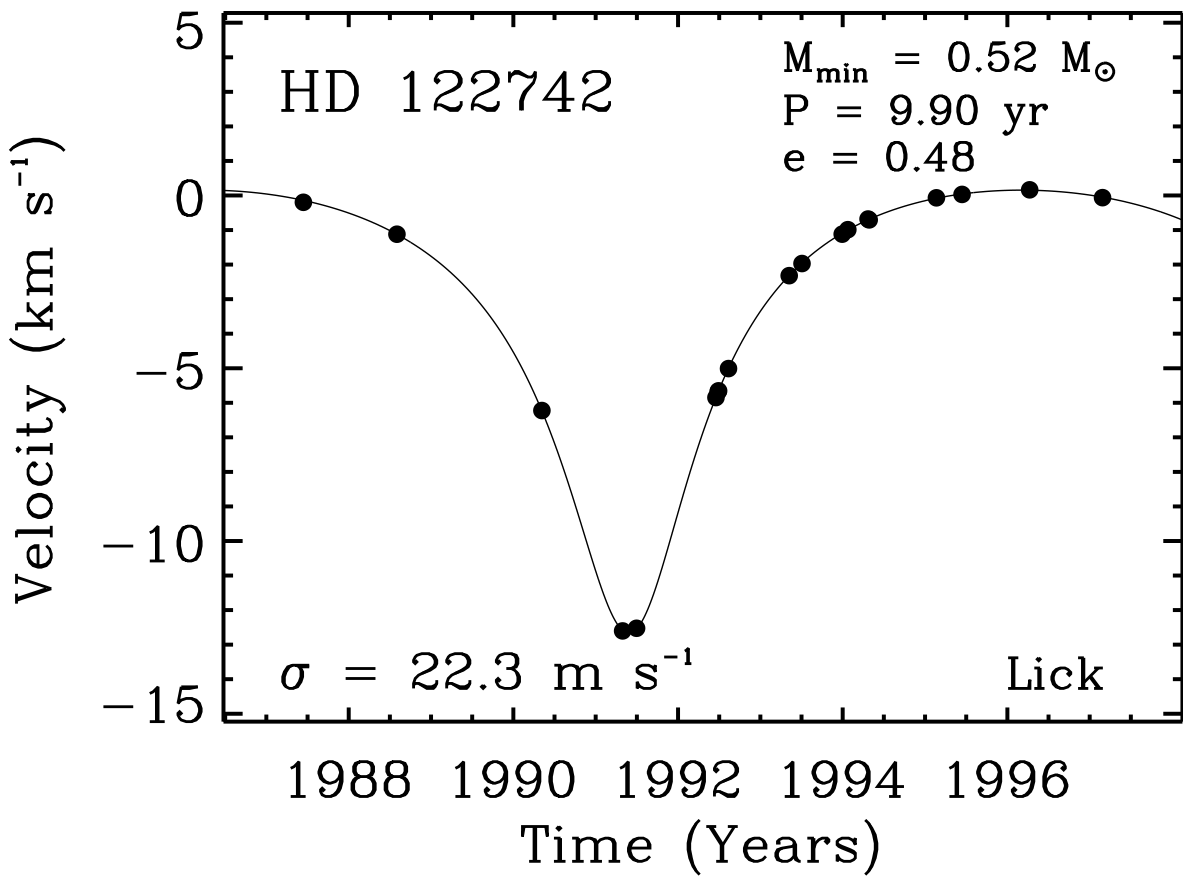


Fig. 15.— Doppler velocities for HD 122742 (G8 V). The solid line is a Keplerian orbital fit with a period of 9.90 yr, a semiamplitude of 6.41 km s^{-1} , and an eccentricity of 0.48, yielding a minimum (M_{\min}) of $0.52 M_{\odot}$ for the companion. The RMS of the Keplerian fit is 22.3 m s^{-1} .

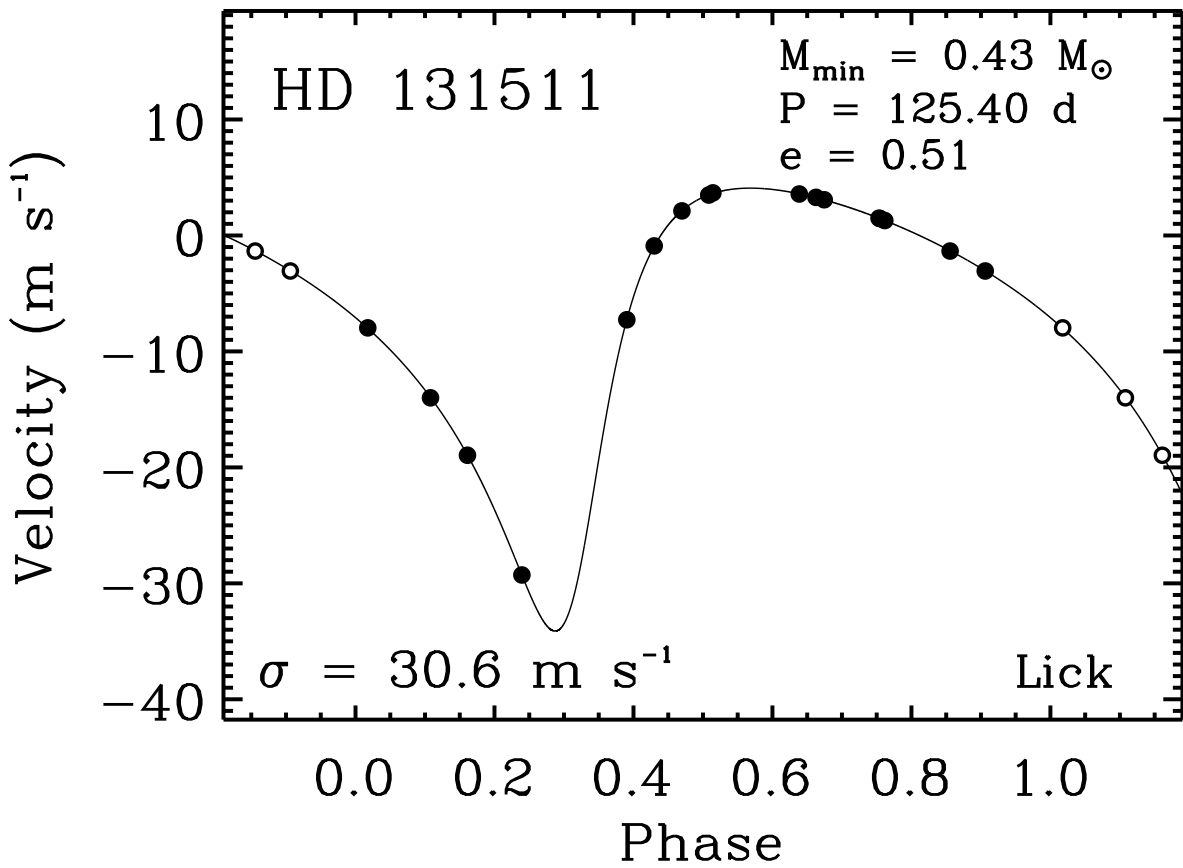


Fig. 16.— Doppler velocities for HD 131511 (K2 V). The solid line is a Keplerian orbital fit with a period of 125.40 d, a semiamplitude of 19.10 km s^{-1} , and an eccentricity of 0.51, yielding a minimum (M_{\min}) of $0.43 M_{\odot}$ for the companion. The RMS of the Keplerian fit is 30.6 m s^{-1} .

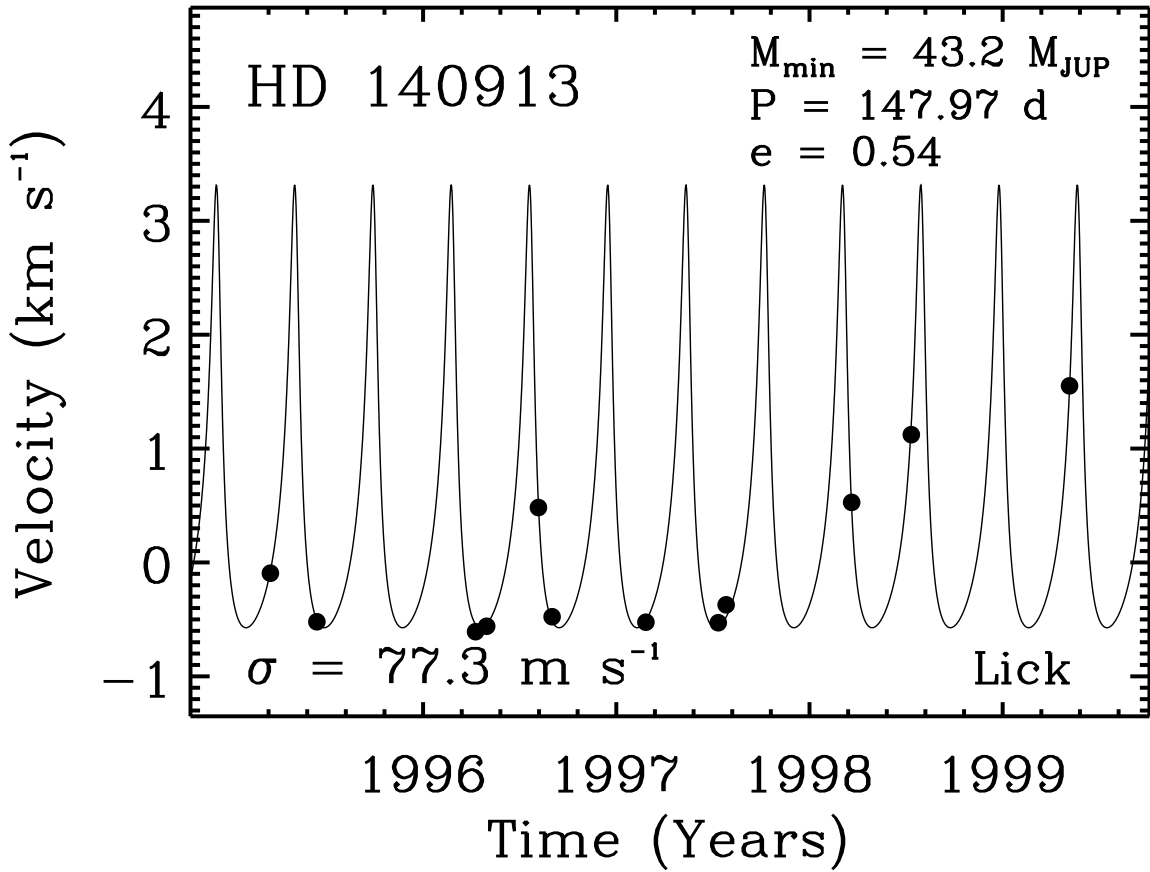


Fig. 17.— Doppler velocities for HD 140913 (G0 V). The solid line is a Keplerian orbital fit with a period of 147.97 d, a semiamplitude of 1.94 km s⁻¹, yielding a minimum (M_{\min}) of 43.2 M_{JUP} for the companion. The eccentricity was fixed to $e = 0.54$ given by Latham et al. (1989) since not enough points were available to constrain the eccentricity. The RMS of the Keplerian fit is 77.3 m s⁻¹.

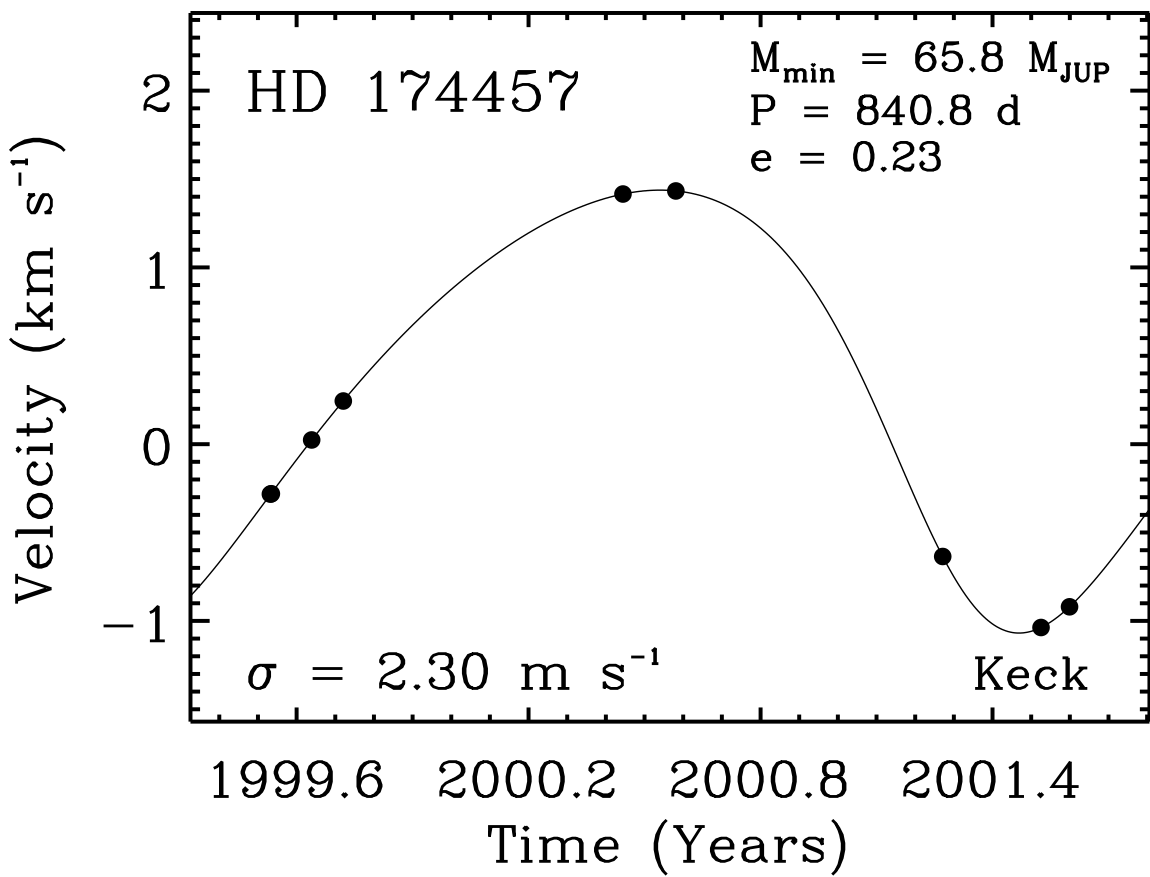


Fig. 18.— Doppler velocities for HD 174457 (F8 V). The solid line is a Keplerian orbital fit with a period of 840.8 d, a semiamplitude of 1.25 km s⁻¹, and an eccentricity of 0.23, yielding a minimum (M_{\min}) of 65.8 M_{JUP} for the companion. The RMS of the Keplerian fit is 2.30 m s⁻¹.

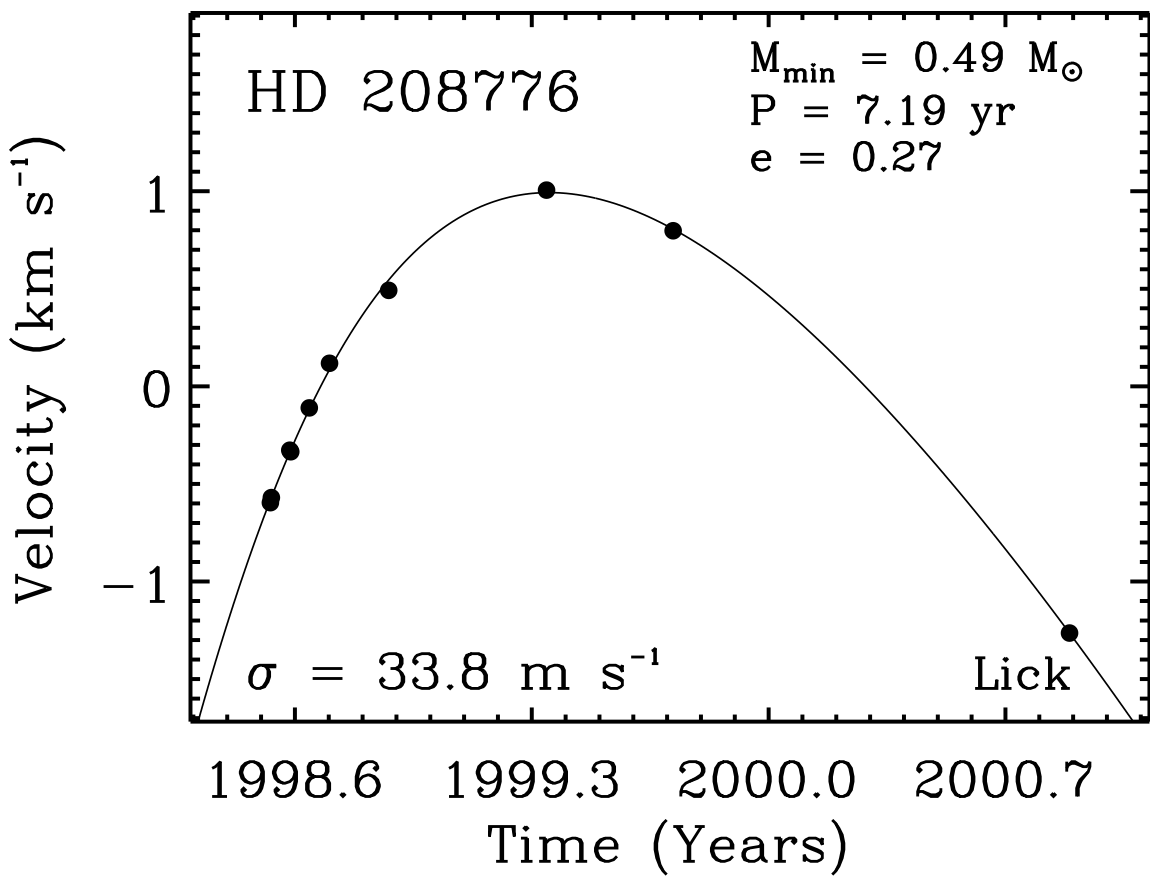


Fig. 19.— Doppler velocities for HD 208776 (G0 V). The solid line is a Keplerian orbital fit with a period of 7.19 yr, a semiamplitude of 5.46 km s⁻¹, and an eccentricity of 0.27, yielding a minimum (M_{\min}) of 0.49 M_{\odot} for the companion. The RMS of the Keplerian fit is 33.8 m s⁻¹.

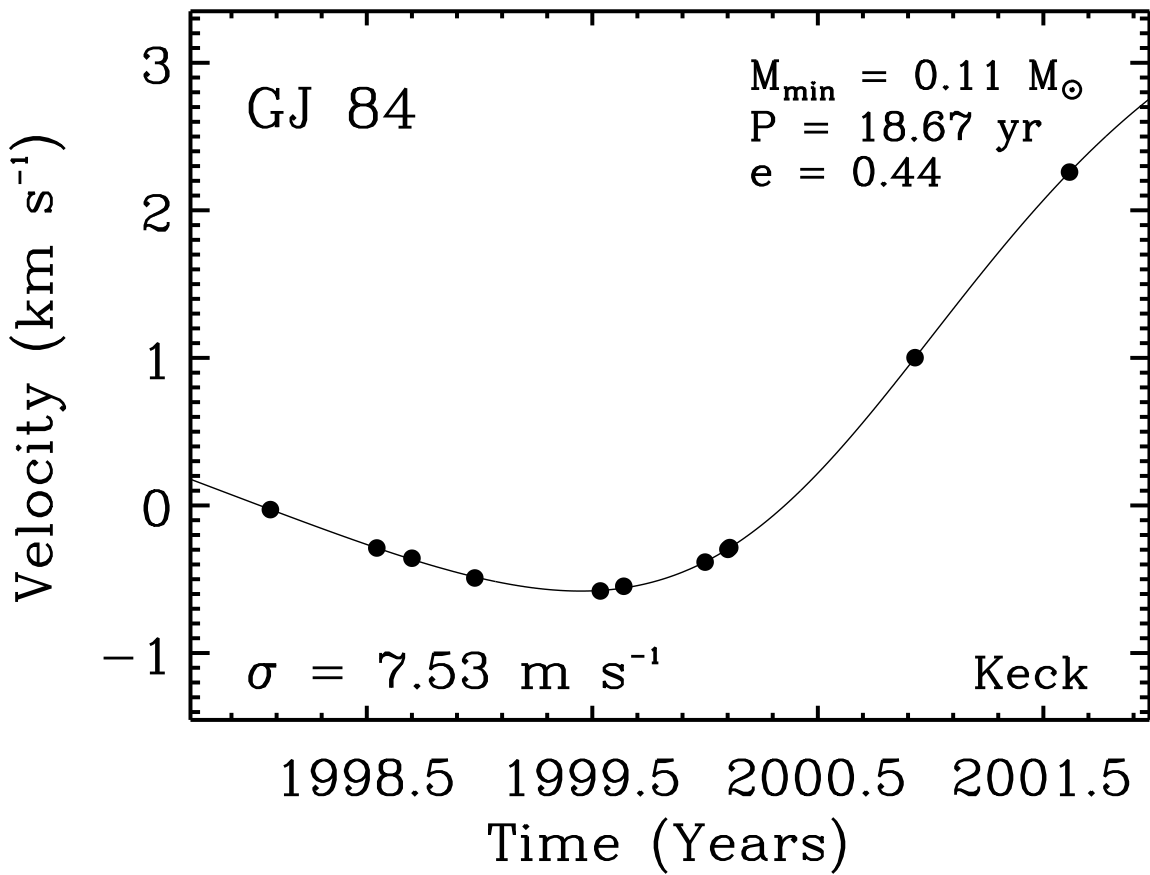


Fig. 20.— Doppler velocities for GJ 84 (M3 V). The solid line is a Keplerian orbital fit with a period of 18.67 yr, a semiamplitude of 2.18 km s⁻¹, and an eccentricity of 0.44, yielding a minimum (M_{\min}) of $0.11 M_{\odot}$ for the companion. The RMS of the Keplerian fit is 7.53 m s^{-1} .

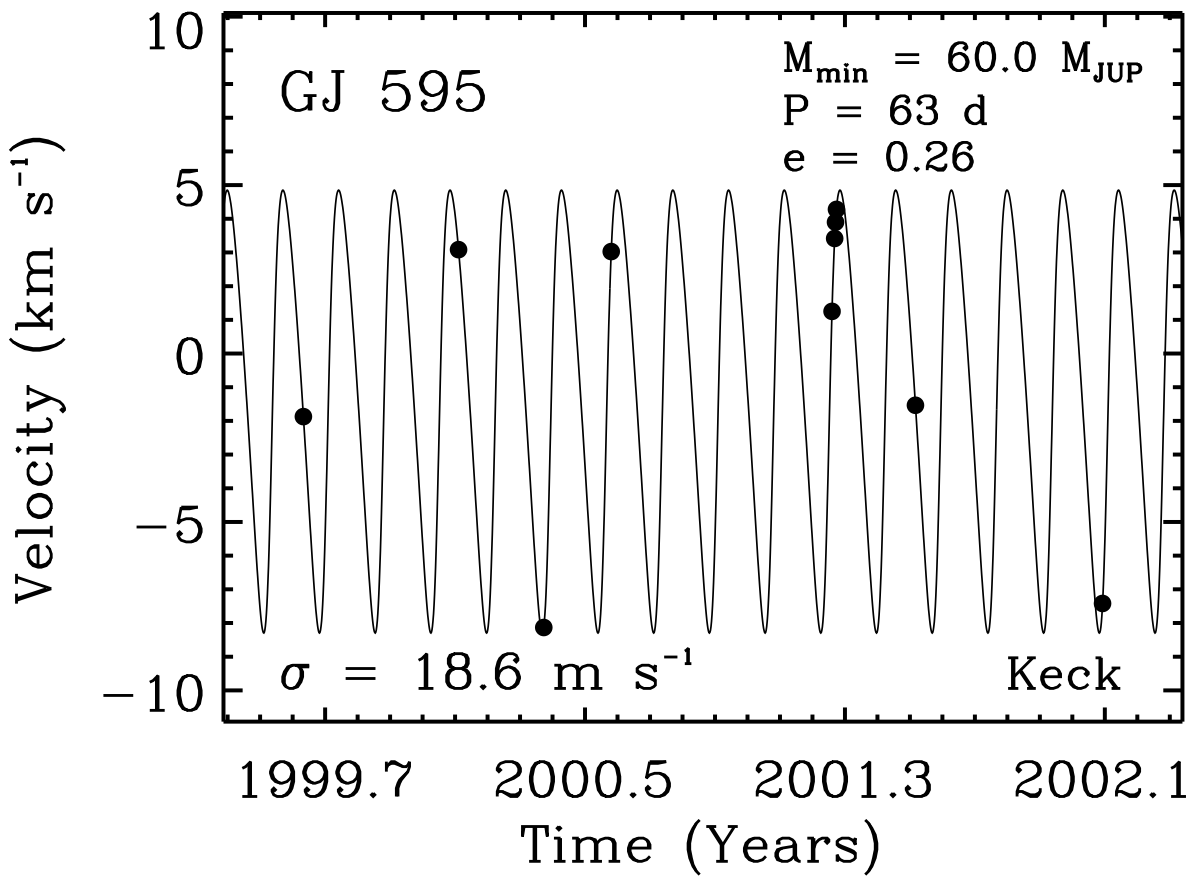


Fig. 21.— Doppler velocities for GJ 595 (M3 V). The solid line is a Keplerian orbital fit with a period of 63 d, a semiamplitude of 6.57 km s^{-1} , and an eccentricity of 0.26, yielding a minimum (M_{\min}) of $60.0 M_{\text{JUP}}$ for the companion. The RMS of the Keplerian fit is 18.6 m s^{-1} .

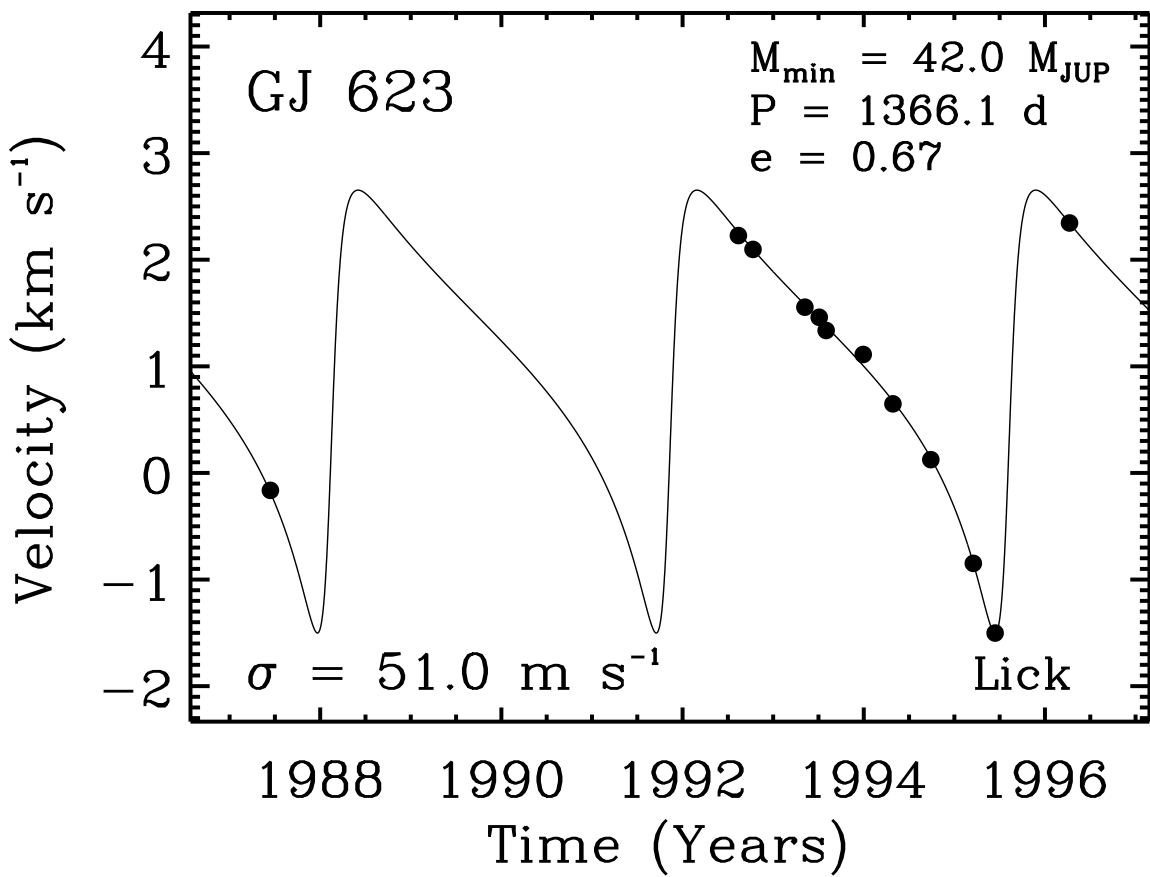


Fig. 22.— Doppler velocities for GJ 623 (M3 V). The solid line is a Keplerian orbital fit with a period of 1366.1 d, a semiamplitude of 2.08 km s⁻¹, and an eccentricity of 0.67, yielding a minimum (M_{\min}) of 42.0 M_{JUP} for the companion. The RMS of the Keplerian fit is 51.0 m s⁻¹.

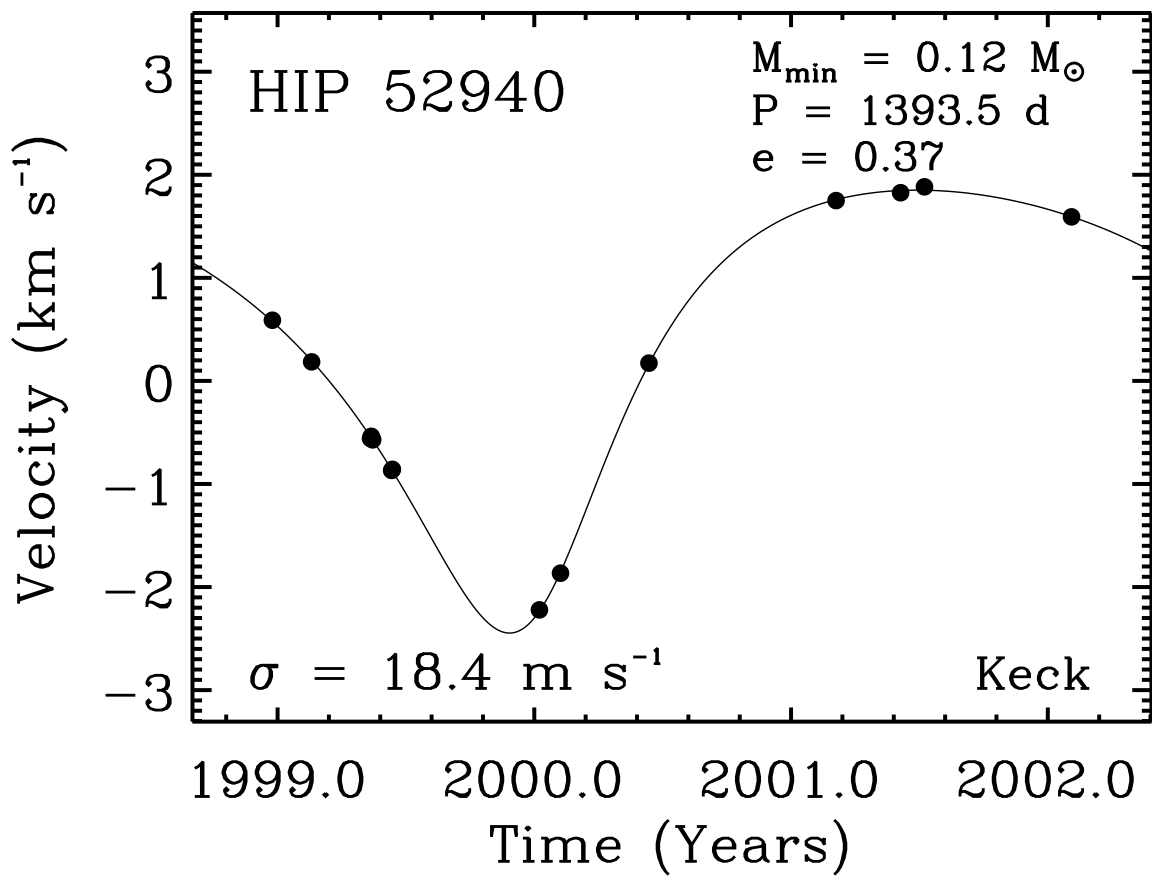


Fig. 23.— Doppler velocities for HIP 52940 (F8 V). The solid line is a Keplerian orbital fit with a period of 1393.5 d, a semiamplitude of 2.15 km s⁻¹, and an eccentricity of 0.37, yielding a minimum (M_{\min}) of 0.12 M_{\odot} for the companion. The RMS of the Keplerian fit is 18.4 m s⁻¹.

Table 1. Radial Velocities of Stable Stars ^a

Primary Name	Alternate Name	Ref (NSO/M)	<JD> (−2,440,000)	ΔT (days)	<RV> (m s ^{−1})
HD 166	HIP 544	NSO	8,783	2,662	−6,537
HD 283	HIP 616	NSO	11,002	1,185	−43,102
HD 377	HIP 682	NSO	11,417	208	1,184
HD 400	HIP 699	NSO	11,137	507	−15,141
HD 531	BD +07 9	NSO	11,419	208	13,460
HD 1326A	GJ 15A	M	9,928	4,656	11,814
HD 1326B	GJ 15B	M	11,294	509	10,976
HD 1388	HIP 1444	NSO	11,016	1,338	28,498
HD 1461	HIP 1499	NSO	11,083	1,184	−10,166
HD 1832	HIP 1813	NSO	11,250	950	−30,550
HD 1835	HIP 1803	NSO	9,123	3,026	−2,405
HD 2025	HIP 1936	NSO	11,218	1,389	3,241
HD 2774	HIP 2497	NSO	11,478	117	−51,566
HD 3074	HIP 2663	NSO	10,955	1,390	29,539
HD 3079	HIP 2712	NSO	11,193	390	−12,347
HD 3651	HIP 3093	NSO	9,708	4,708	−32,961
HD 3674	HIP 3119	NSO	11,161	514	166
HD 3765	HIP 3206	NSO	11,151	1,294	−63,202
HD 3861	HIP 3236	NSO	11,055	105	−14,796
HD 4203	HIP 3502	NSO	12,020	431	−14,140
HD 4208	HIP 3479	NSO	11,345	1,427	56,726
HD 4256	HIP 3535	NSO	11,069	1,177	9,460
HD 4307	HIP 3559	NSO	11,303	1,390	−10,349
HD 4614	HIP 3821	NSO	9,380	4,080	8,314
HD 4614B	GJ 34B	M	10,036	1,860	11,293
HD 4628	HIP 3765	NSO	9,262	3,747	−10,230
HD 4915	HIP 3979	NSO	11,348	291	−3,742
HD 5065	HIP 4127	NSO	11,336	510	−73,844
HD 5133	HIP 4148	NSO	11,470	96	−13,067
HD 5372	HIP 4393	NSO	11,325	950	596
HD 6101	HIP 4849	NSO	11,041	58	22,170

Table 1—Continued

Primary Name	Alternate Name	Ref (NSO/M)	<JD> (−2,440,000)	ΔT (days)	<RV> (m s ^{−1})
HD 6611	HIP 5276	NSO	11,027	0	−6,068
HD 6734	HIP 5315	NSO	11,130	1,426	−94,511
HD 7047	HIP 5534	NSO	11,128	418	9,264
HD 7228	HIP 5682	NSO	11,450	509	−20,538
HD 7590	HIP 5944	NSO	11,425	27	−13,073
HD 7727	HIP 5985	NSO	11,262	514	5,898
HD 8262	HIP 6405	NSO	11,290	507	5,636
HD 8389	HIP 6456	NSO	10,869	1,177	34,647
HD 8574	HIP 6643	NSO	11,328	1,161	18,886
HD 8648	HIP 6653	NSO	11,441	987	923
HD 8763	HIP 6732	NSO	11,487	117	−42,532
HD 8941	HIP 6869	NSO	11,171	419	9,132
HD 9224	HIP 7090	NSO	11,174	507	14,937
HD 9280	HIP 7080	NSO	11,172	3	41,861
HD 9331	HIP 7221	NSO	11,933	246	−20,086
HD 9407	HIP 7339	NSO	11,248	538	−33,291
HD 9562	HIP 7276	NSO	11,071	1,390	−14,989
HD 9826	HIP 7513	NSO	8,547	2,576	−28,674
HD 9986	HIP 7585	NSO	11,276	987	−21,047
HD 10002	HIP 7539	NSO	10,973	1,119	11,562
HD 10086	HIP 7734	NSO	11,297	514	2,143
HD 10126	HIP 7733	NSO	11,301	293	56,156
HD 10145	HIP 7902	NSO	11,098	1,121	17,838
HD 10436	HIP 8070	NSO	11,469	184	−50,957
HD 10476	HIP 7981	NSO	10,921	1,387	−33,647
HD 10697	HIP 8159	NSO	11,044	1,044	−46,022
HD 10700	HIP 8102	NSO	9,838	5,053	−16,619
HD 10780	HIP 8362	NSO	11,404	384	2,764
HD 11020	HIP 8346	NSO	10,999	1,081	22,786
HD 11226	HIP 8548	NSO	11,310	513	10,314
HD 11505	HIP 8798	NSO	11,279	420	−16,470

Table 1—Continued

Primary Name	Alternate Name	Ref (NSO/M)	<JD> (−2,440,000)	ΔT (days)	<RV> (m s ^{−1})
HD 11964	HIP 9094	NSO	11,109	1,391	−9,366
HD 12051	HIP 9269	NSO	11,097	1,125	−35,102
HD 12235	HIP 9353	NSO	9,727	3,965	−18,434
HD 12414	HIP 9473	NSO	10,997	301	15,898
HD 12661	HIP 9683	NSO	11,463	944	−47,310
HD 12846	HIP 9829	NSO	11,435	595	−4,662
HD 13043	HIP 9911	NSO	11,030	1,043	−39,333
HD 13507	HIP 10321	NSO	11,141	397	6,172
HD 13531	HIP 10339	NSO	10,979	245	7,203
HD 13579	HIP 10531	NSO	11,339	293	−12,723
HD 13612B	HIP 10303	NSO	11,076	1,184	−5,337
HD 13825	HIP 10505	NSO	11,270	432	−2,237
HD 13931	HIP 10626	NSO	11,265	748	30,538
HD 14412	HIP 10798	NSO	11,006	1,391	7,383
HD 15176	HIP 11432	NSO	11,494	145	−41,783
HD 15335	HIP 11548	NSO	11,031	1,219	41,202
HD 16141	HIP 12048	NSO	11,067	1,008	−50,971
HD 16160	HIP 12114	NSO	9,351	3,608	25,766
HD 16397	HIP 12306	NSO	11,060	1,082	−99,660
HD 16623	HIP 12364	NSO	11,088	829	17,502
HD 16895	HIP 12777	NSO	8,930	2,937	24,453
HD 17190	HIP 12926	NSO	11,146	1,186	14,138
HD 17230	HIP 12929	NSO	11,443	386	11,061
HD 17332	HIP 13027	NSO	11,481	140	4,427
HD 17660	HIP 13258	NSO	11,396	324	−28,904
HD 17925	HIP 13402	NSO	9,385	4,084	18,068
HD 18143	HIP 13642	NSO	11,079	1,186	31,950
HD 18144	HIP 13601	NSO	11,418	386	−1,329
HD 18449	HIP 13905	NSO	11,487	118	−37,021
HD 18632	HIP 13976	NSO	11,263	540	28,826
HD 18803	HIP 14150	NSO	11,210	1,426	9,878

Table 1—Continued

Primary Name	Alternate Name	Ref (NSO/M)	<JD> (−2,440,000)	ΔT (days)	<RV> (m s ^{−1})
HD 18907	HIP 14086	NSO	11,172	2	42,718
HD 19034	HIP 14241	NSO	11,082	1,186	−20,344
HD 19308	HIP 14532	NSO	11,234	714	32,723
HD 19373	HIP 14632	NSO	7,328	532	49,449
HD 19467	HIP 14501	NSO	10,996	1,217	6,936
HD 19994	HIP 14954	NSO	9,069	4,758	19,331
HD 20165	HIP 15099	NSO	11,070	1,186	−16,676
HD 20619	HIP 15442	NSO	10,941	1,178	22,689
HD 20630	HIP 15457	NSO	7,834	1,847	19,021
HD 21019	HIP 15776	NSO	10,991	1,178	41,630
HD 21197	HIP 15919	NSO	11,145	1,186	−13,107
HD 21313	HIP 16107	NSO	11,901	182	−20,017
HD 21847	HIP 16517	NSO	11,263	714	30,033
HD 22049	HIP 16537	NSO	7,147	177	16,332
HD 22072	HIP 16641	NSO	11,070	1,463	11,050
HD 22484	HIP 16852	NSO	8,391	2,301	28,080
HD 22879	HIP 17147	NSO	11,076	1,427	120,356
HD 23249	HIP 17378	NSO	11,162	1,330	−6,295
HD 23356	HIP 17420	NSO	11,220	501	25,287
HD 23439	HIP 17666	NSO	11,102	1,119	50,704
HD 24040	HIP 17960	NSO	11,278	954	−9,423
HD 24213	HIP 18106	NSO	11,181	712	−39,608
HD 24238	HIP 18324	NSO	11,038	1,088	38,809
HD 24341	HIP 18309	NSO	11,038	1,088	142,798
HD 24365	HIP 18208	NSO	11,092	1,088	19,278
HD 24451	HIP 18774	NSO	11,404	354	17,670
HD 24496	HIP 18267	NSO	11,236	954	18,936
HD 24727	HIP 18388	NSO	11,304	954	−18,140
HD 24892	HIP 18432	NSO	10,952	1,217	45,410
HD 24916	HIP 18512	NSO	11,245	1,427	3,540
HD 25069	HIP 18606	NSO	11,133	1,427	38,484

Table 1—Continued

Primary Name	Alternate Name	Ref (NSO/M)	<JD> (−2,440,000)	ΔT (days)	<RV> (m s ^{−1})
HD 25665	HIP 19422	NSO	11,436	29	−13,546
HD 25680	HIP 19076	NSO	9,509	4,084	24,034
HD 25723	HIP 19011	NSO	11,490	144	26,748
HD 25918	HIP 19301	NSO	11,538	5	−36,198
HD 26151	HIP 19232	NSO	11,416	412	−6,804
HD 26161	HIP 19428	NSO	11,236	714	12,924
HD 26162	HIP 19388	NSO	11,497	116	24,776
HD 26767	HIP 19786	NSO	11,728	564	38,288
HD 26794	HIP 19788	NSO	10,980	1,131	56,573
HD 26965	HIP 19849	NSO	7,657	1,845	−42,331
HD 28005	HIP 20800	NSO	11,231	714	34,768
HD 28187	HIP 20638	NSO	10,990	1,215	18,321
HD 28343	HIP 20917	M	11,476	356	−35,073
HD 28344	HIP 20899	NSO	11,524	171	39,145
HD 28676	HIP 21158	NSO	11,305	361	6,671
HD 28946	HIP 21272	NSO	11,395	386	−46,353
HD 29150	HIP 21436	NSO	11,396	386	−6,615
HD 29528	HIP 21703	NSO	11,901	182	−18,922
HD 29883	HIP 21988	NSO	11,359	385	17,843
HD 30562	HIP 22336	NSO	11,370	293	77,189
HD 30708	HIP 22576	NSO	11,209	714	−55,738
HD 31253	HIP 22826	NSO	11,345	954	12,184
HD 31560	HIP 22907	NSO	11,162	1,217	6,203
HD 31966	HIP 23286	NSO	11,239	743	−18,058
HD 32147	HIP 23311	NSO	9,858	4,085	21,552
HD 32923	HIP 23835	NSO	11,305	388	20,558
HD 32963	HIP 23884	NSO	11,235	715	−62,435
HD 33021	HIP 23852	NSO	11,070	1,216	−22,300
HD 33632	HIP 24332	NSO	11,182	708	−1,707
HD 33636	HIP 24205	NSO	11,411	954	5,714
HD 33793	HIP 24186	M	11,376	410	245,194

Table 1—Continued

Primary Name	Alternate Name	Ref (NSO/M)	<JD> (−2,440,000)	ΔT (days)	<RV> (m s ^{−1})
HD 34411	HIP 24813	NSO	7,970	1,859	66,511
HD 34445	HIP 24681	NSO	11,256	743	−78,949
HD 34575	HIP 25094	NSO	11,731	357	−23,520
HD 34721	HIP 24786	NSO	11,041	1,217	40,448
HD 34745	HIP 24864	NSO	11,255	743	35,376
HD 35627	HIP 25388	NSO	11,208	713	27,267
HD 35681	HIP 25580	NSO	11,195	702	12,136
HD 35974	HIP 25490	NSO	11,017	1,162	76,683
HD 36003	HIP 25623	NSO	11,214	1,215	−55,527
HD 36395	HIP 25878	M	10,194	4,537	8,665
HD 37124	HIP 26381	NSO	11,203	1,164	−23,076
HD 37213	HIP 26273	NSO	11,088	1,163	12,464
HD 37394	HIP 26779	NSO	9,701	2,486	1,207
HD 37588	HIP 26689	NSO	10,857	0	−58,276
HD 37962	HIP 26737	NSO	10,899	862	3,133
HD 38230	HIP 27207	NSO	11,058	1,133	−29,177
HD 38529	HIP 27253	NSO	11,273	1,374	30,210
HD 38858	HIP 27435	NSO	11,017	1,133	31,543
HD 39715	HIP 27918	NSO	11,461	386	−33,797
HD 39881	HIP 28066	NSO	11,025	1,220	333
HD 40397	HIP 28267	NSO	11,113	713	143,621
HD 40650	HIP 28634	NSO	11,030	343	−76,840
HD 40979	HIP 28767	NSO	10,955	344	32,542
HD 42250	HIP 29761	NSO	10,908	1,119	19,715
HD 42581	HIP 29295	M	10,801	1,579	4,724
HD 42618	HIP 29432	NSO	11,054	1,220	−53,501
HD 43523	HIP 30023	NSO	11,261	709	−16,172
HD 43745	HIP 29843	NSO	10,964	1,187	−2,716
HD 43947	HIP 30067	NSO	11,181	714	40,545
HD 44420	HIP 30243	NSO	11,745	464	−531
HD 44985	HIP 30552	NSO	11,227	714	32,253

Table 1—Continued

Primary Name	Alternate Name	Ref (NSO/M)	<JD> (−2,440,000)	ΔT (days)	<RV> (m s ^{−1})
HD 45067	HIP 30545	NSO	11,118	1,166	47,280
HD 45184	HIP 30503	NSO	10,940	1,220	−3,856
HD 45350	HIP 30860	NSO	11,819	431	−20,727
HD 45391	HIP 30862	NSO	11,459	472	−5,388
HD 45588	HIP 30711	NSO	10,911	1,187	35,856
HD 46375	HIP 31246	NSO	11,491	514	−1,032
HD 47127	HIP 31660	NSO	11,279	750	49,694
HD 47157	HIP 31655	NSO	11,549	46	25,330
HD 47752	HIP 32010	NSO	11,585	90	−44,253
HD 48682	HIP 32480	NSO	8,280	2,301	−23,933
HD 48938	HIP 32322	NSO	10,927	1,134	−10,563
HD 49674	HIP 32916	NSO	11,963	182	12,045
HD 49736	HIP 32874	NSO	11,048	708	6,687
HD 50281	HIP 32984	NSO	10,546	2,276	−7,082
HD 50499	HIP 32970	NSO	10,971	1,167	36,793
HD 50554	HIP 33212	NSO	11,219	709	−3,888
HD 50692	HIP 33277	NSO	10,965	1,119	−15,023
HD 50806	HIP 33094	NSO	10,870	1,187	72,388
HD 51219	HIP 33382	NSO	11,074	737	−8,071
HD 51866	HIP 33852	NSO	11,060	1,120	−21,624
HD 52265	HIP 33719	NSO	11,370	745	53,810
HD 52456	HIP 33848	NSO	11,325	514	−11,909
HD 52711	HIP 34017	NSO	9,614	4,502	24,604
HD 53665	HIP 34239	NSO	11,232	747	−14,703
HD 55575	HIP 35136	NSO	11,386	476	84,809
HD 56124	HIP 35265	NSO	11,324	685	22,526
HD 56274	HIP 35139	NSO	10,929	1,125	66,663
HD 56303	HIP 35209	NSO	11,164	705	8,150
HD 58781	HIP 36249	NSO	11,285	744	5,013
HD 59747	HIP 36704	NSO	11,441	472	−15,744
HD 60491	HIP 36827	NSO	11,385	410	−9,667

Table 1—Continued

Primary Name	Alternate Name	Ref (NSO/M)	<JD> (−2,440,000)	ΔT (days)	<RV> (m s ^{−1})
HD 61606	HIP 37349	NSO	11, 255	1, 163	−18, 210
HD 63077	HIP 37853	NSO	10, 415	97	106, 159
HD 63433	HIP 38228	NSO	11, 232	703	−15, 888
HD 63754	HIP 38216	NSO	10, 867	1, 132	44, 973
HD 64090	HIP 38541	NSO	10, 968	416	−234, 268
HD 65277	HIP 38931	NSO	11, 005	1, 120	−4, 417
HD 65583	HIP 39157	NSO	10, 958	1, 133	14, 832
HD 66171	HIP 39822	NSO	10, 944	1, 119	36, 412
HD 66428	HIP 39417	NSO	11, 926	92	44, 140
HD 67228	HIP 39780	NSO	11, 431	456	−36, 012
HD 67458	HIP 39710	NSO	11, 047	1, 120	−15, 686
HD 67767	HIP 40023	NSO	11, 038	1, 261	−44, 318
HD 68017	HIP 40118	NSO	11, 068	1, 218	29, 575
HD 68168	HIP 40133	NSO	11, 144	746	9, 162
HD 68978	HIP 40283	NSO	10, 937	1, 119	51, 696
HD 69809	HIP 40761	NSO	11, 743	422	17, 534
HD 69897	HIP 40843	NSO	8, 392	2, 250	32, 733
HD 70843	HIP 41226	NSO	11, 267	795	−13, 087
HD 71148	HIP 41484	NSO	11, 177	798	−32, 342
HD 71334	HIP 41317	NSO	11, 120	1, 124	17, 286
HD 71479	HIP 41479	NSO	11, 255	742	60, 217
HD 71881	HIP 41844	NSO	11, 046	745	13, 629
HD 72659	HIP 42030	NSO	11, 255	742	−18, 253
HD 72673	HIP 41926	NSO	10, 792	808	14, 785
HD 72760	HIP 42074	NSO	11, 386	798	34, 928
HD 73344	HIP 42403	NSO	11, 161	468	6, 097
HD 73350	HIP 42333	NSO	11, 052	412	35, 370
HD 73667	HIP 42499	NSO	10, 981	1, 091	−12, 088
HD 74014	HIP 42634	NSO	11, 462	475	−17, 089
HD 75332	HIP 43410	NSO	11, 173	469	4, 256
HD 75732	HIP 43587	NSO	9, 301	2, 513	27, 351

Table 1—Continued

Primary Name	Alternate Name	Ref (NSO/M)	<JD> (−2,440,000)	ΔT (days)	<RV> (m s ^{−1})
HD 76151	HIP 43726	NSO	9,469	2,926	32,002
HD 76752	HIP 44089	NSO	11,358	798	−12,577
HD 76909	HIP 44137	NSO	11,725	429	3,045
HD 77407	HIP 44458	NSO	10,843	23	4,827
HD 78366	HIP 44897	NSO	9,485	3,286	26,120
HD 79210	HIP 45343	M	11,045	974	11,142
HD 79211	HIP 120005	M	11,077	974	12,495
HD 80367	HIP 45737	NSO	11,416	412	51,009
HD 82106	HIP 46580	NSO	10,970	323	29,836
HD 83443	HIP 47202	NSO	11,982	167	28,994
HD 84035	HIP 47690	NSO	10,989	1,121	−12,225
HD 84737	HIP 48113	NSO	8,233	1,919	4,900
HD 85725	HIP 48468	NSO	10,726	752	61,610
HD 86728	HIP 49081	NSO	8,649	2,716	55,956
HD 87359	HIP 49350	NSO	11,113	737	−260
HD 87424	HIP 49366	NSO	11,316	380	−12,133
HD 87836	HIP 49680	NSO	11,568	96	−42,188
HD 87883	HIP 49699	NSO	11,311	379	9,254
HD 88072	HIP 49756	NSO	11,062	737	−17,886
HD 88218	HIP 49769	NSO	11,010	1,261	36,652
HD 88230	HIP 49908	M	8,883	2,897	−25,729
HD 88371	HIP 49942	NSO	11,006	1,089	82,497
HD 88725	HIP 50139	NSO	10,999	1,217	−22,045
HD 88986	HIP 50316	NSO	10,818	809	29,019
HD 89269	HIP 50505	NSO	10,979	1,164	−7,551
HD 89307	HIP 50473	NSO	11,074	358	23,011
HD 89391	HIP 50478	NSO	11,167	1,119	29,607
HD 90125	HIP 50939	NSO	11,054	1,286	−13,937
HD 90156	HIP 50921	NSO	10,899	1,162	26,934
HD 90711	HIP 51257	NSO	11,012	1,089	29,940
HD 90722	HIP 51258	NSO	11,703	423	39,984

Table 1—Continued

Primary Name	Alternate Name	Ref (NSO/M)	<JD> (−2,440,000)	ΔT (days)	<RV> (m s ^{−1})
HD 90839	HIP 51459	NSO	8,584	3,023	8,529
HD 90875	HIP 51468	NSO	11,381	383	4,948
HD 91204	HIP 51579	NSO	11,853	432	−8,875
HD 91638	HIP 51784	NSO	11,056	381	−4,751
HD 92788	HIP 52409	NSO	11,535	924	−4,529
HD 92945	HIP 52462	NSO	11,323	1,218	22,856
HD 93745	HIP 52888	NSO	11,019	1,218	37,947
HD 94765	HIP 53486	NSO	11,599	93	5,525
HD 95128	HIP 53721	NSO	9,800	4,241	11,235
HD 95650	HIP 53985	M	11,816	423	−13,899
HD 95735	HIP 54035	M	10,213	4,748	−84,689
HD 96418	HIP 54347	NSO	11,101	411	−8,013
HD 96574	HIP 54383	NSO	11,271	57	36,055
HD 96700	HIP 54400	NSO	10,995	1,261	12,769
HD 97004	HIP 54614	NSO	11,361	293	5,352
HD 97037	HIP 54582	NSO	11,294	709	−15,914
HD 97101	GJ 414A	NSO	10,384	2,902	−16,376
HD 97101B	GJ 414B	M	10,307	1,930	−15,333
HD 97334	HIP 54745	NSO	9,429	3,273	−3,662
HD 97343	HIP 54704	NSO	11,051	1,261	39,794
HD 97658	HIP 54906	NSO	10,965	1,088	−1,654
HD 98281	HIP 55210	NSO	11,044	1,121	13,330
HD 98618	HIP 55459	NSO	11,242	865	7,058
HD 98697	HIP 55455	NSO	11,441	453	−14,312
HD 99109	HIP 55664	NSO	11,478	534	32,997
HD 99491	HIP 55846	NSO	11,047	1,286	4,190
HD 99492	HIP 55848	NSO	11,110	1,243	3,726
HD 100180	HIP 56242	NSO	11,017	1,284	−4,854
HD 100623	HIP 56452	NSO	11,003	1,162	−21,959
HD 101177	HIP 56809	NSO	11,461	386	−16,912
HD 101259	HIP 56830	NSO	11,077	1,121	96,905

Table 1—Continued

Primary Name	Alternate Name	Ref (NSO/M)	<JD> (−2,440,000)	ΔT (days)	<RV> (m s ^{−1})
HD 101501	HIP 56997	NSO	7,992	2,213	−5,565
HD 102158	HIP 57349	NSO	11,009	1,121	28,122
HD 102634	HIP 57629	NSO	11,099	381	1,254
HD 102870	HIP 57757	NSO	7,466	1,058	4,448
HD 103095	HIP 57939	NSO	11,289	153	−98,073
HD 103432	HIP 58067	NSO	11,033	1,241	6,079
HD 103932	HIP 58345	NSO	11,114	1,218	48,499
HD 104067	HIP 58451	NSO	11,247	1,218	15,021
HD 104526	HIP 58698	NSO	10,539	143	4,635
HD 104556	HIP 58708	NSO	11,057	1,240	−10,678
HD 104800	HIP 58843	NSO	11,820	547	9,989
HD 105113	HIP 59021	NSO	11,070	1,218	31,871
HD 105405	HIP 59175	NSO	11,412	325	2,196
HD 105590	HIP 59272	NSO	10,733	494	1,976
HD 105618	HIP 59278	NSO	11,957	219	7,466
HD 105631	HIP 59280	NSO	11,033	1,240	−2,428
HD 106116	HIP 59532	NSO	11,063	1,241	14,543
HD 106156	HIP 59572	NSO	11,063	1,240	−7,415
HD 107148	HIP 60081	NSO	11,890	548	25,216
HD 107705	HIP 60353	NSO	11,278	797	4,759
HD 108510	HIP 60816	NSO	11,207	0	6,888
HD 108874	HIP 61028	NSO	11,521	339	−30,137
HD 109358	HIP 61317	NSO	11,735	480	6,259
HD 110315	HIP 61901	NSO	11,108	1,242	24,604
HD 110537	HIP 62039	NSO	11,386	748	35,461
HD 111031	HIP 62345	NSO	11,051	1,243	−20,458
HD 111066	HIP 62349	NSO	11,351	330	6,407
HD 111398	HIP 62536	NSO	11,411	331	3,154
HD 111484	HIP 62596	NSO	11,408	721	−20,643
HD 111484B	SAO 119612	NSO	11,387	721	−19,377
HD 111515	HIP 62607	NSO	11,059	1,243	2,548

Table 1—Continued

Primary Name	Alternate Name	Ref (NSO/M)	<JD> (−2,440,000)	ΔT (days)	<RV> (m s ^{−1})
HD 111631	HIP 62687	M	11,901	517	5,041
HD 112257	HIP 63048	NSO	11,044	473	−39,428
HD 114174	HIP 64150	NSO	11,083	1,119	24,002
HD 114710	HIP 64394	NSO	7,397	1,058	5,295
HD 114729	HIP 64459	NSO	11,380	1,244	64,925
HD 114783	HIP 64457	NSO	11,551	772	−12,012
HD 114946	HIP 64577	NSO	11,118	1,242	−48,181
HD 115383	HIP 64792	NSO	8,623	2,511	−27,138
HD 115589	HIP 64905	NSO	11,434	505	−21,614
HD 115617	HIP 64924	NSO	9,770	0	−7,850
HD 116442	HIP 65352	NSO	11,301	1,242	28,421
HD 116443	HIP 65355	NSO	11,155	1,242	27,416
HD 117207	HIP 65808	NSO	11,199	1,240	−17,476
HD 117936	HIP 66147	NSO	11,404	720	−6,086
HD 118914	HIP 66621	NSO	11,950	307	16,460
HD 119850	HIP 67155	M	10,336	2,856	15,809
HD 120066	HIP 67246	NSO	11,205	1,241	−30,561
HD 120467	HIP 67487	NSO	11,252	1,157	−37,806
HD 120476	HIP 67422	NSO	11,492	392	−20,380
HD 121560	HIP 68030	NSO	11,016	23	−10,532
HD 122064	HIP 68184	NSO	11,958	548	−26,471
HD 122120	HIP 68337	NSO	11,130	1,157	−57,444
HD 122303	HIP 68469	M	11,497	172	−25,813
HD 122652	HIP 68593	NSO	11,177	675	1,409
HD 124106	HIP 69357	NSO	11,117	1,396	3,288
HD 124292	HIP 69414	NSO	11,104	474	37,773
HD 124642	HIP 69526	NSO	11,585	89	−16,242
HD 124694	HIP 69518	NSO	11,016	22	−14,644
HD 125184	HIP 69881	NSO	11,184	1,403	−12,377
HD 125455	HIP 70016	NSO	11,154	1,404	−9,806
HD 126053	HIP 70319	NSO	10,208	4,746	−19,241

Table 1—Continued

Primary Name	Alternate Name	Ref (NSO/M)	<JD> (−2,440,000)	ΔT (days)	<RV> (m s ^{−1})
HD 126614	HIP 70623	NSO	11,485	480	−33,086
HD 126961	HIP 70782	NSO	11,050	202	−5,839
HD 127334	HIP 70873	NSO	11,129	533	−405
HD 128167	HIP 71284	NSO	8,333	2,080	141
HD 128311	HIP 71395	NSO	11,392	696	−9,569
HD 128428	HIP 71462	NSO	11,063	795	−42,074
HD 129010	HIP 71774	NSO	11,149	1,158	−8,137
HD 129191	HIP 71803	NSO	11,827	479	12,685
HD 130087	HIP 72190	NSO	11,835	483	−15,673
HD 130307	HIP 72312	NSO	11,218	1,429	12,864
HD 130322	HIP 72339	NSO	12,038	407	−12,441
HD 130871	HIP 72577	NSO	11,147	1,429	−32,159
HD 130948	HIP 72567	NSO	9,090	3,698	−2,502
HD 130992	HIP 72688	NSO	11,256	1,134	−57,160
HD 131117	HIP 72772	NSO	11,105	1,242	−28,834
HD 131156A	GJ 566A	NSO	7,325	1,157	1,303
HD 131156B	GJ 566B	NSO	9,090	3,609	3,274
HD 131509	HIP 72830	NSO	11,090	1,133	−44,625
HD 131977	HIP 73184	NSO	10,272	1,407	26,961
HD 132142	HIP 73005	NSO	11,094	1,158	−14,771
HD 132375	HIP 73309	NSO	11,139	624	−24,370
HD 133161	HIP 73593	NSO	11,181	796	−32,628
HD 134044	HIP 73941	NSO	11,222	624	−5,874
HD 134439	HIP 74235	NSO	11,090	820	310,084
HD 134440	HIP 74234	NSO	11,365	692	310,614
HD 134987	HIP 74500	NSO	10,962	952	5,038
HD 135101	HIP 74432	NSO	11,259	1,480	−38,921
HD 135599	HIP 74702	NSO	11,108	468	−3,149
HD 136442	HIP 75101	NSO	11,483	720	−46,935
HD 136654	HIP 75104	NSO	11,020	21	−27,029
HD 136713	HIP 75253	NSO	11,090	1,428	−6,037

Table 1—Continued

Primary Name	Alternate Name	Ref (NSO/M)	<JD> (−2,440,000)	ΔT (days)	<RV> (m s ^{−1})
HD 136834	HIP 75266	NSO	10,982	1,403	−26,374
HD 136923	HIP 75277	NSO	11,196	798	−7,042
HD 136925	HIP 75281	NSO	11,253	842	−48,942
HD 137778	HIP 75722	NSO	11,234	1,479	7,752
HD 138549	HIP 76200	NSO	11,100	1,158	12,024
HD 138573	HIP 76114	NSO	11,221	625	−35,691
HD 138776	HIP 76228	NSO	11,509	368	10,674
HD 139323	HIP 76375	NSO	11,092	1,134	−67,101
HD 139457	HIP 76543	NSO	11,427	338	37,708
HD 139477	HIP 76315	NSO	11,387	453	−8,893
HD 141004	HIP 77257	NSO	8,789	3,560	−66,416
HD 141103	HIP 77335	NSO	11,106	358	−48,258
HD 142373	HIP 77760	NSO	8,418	3,561	−56,107
HD 142860	HIP 78072	NSO	7,746	1,327	6,544
HD 143291	HIP 78241	NSO	11,065	1,428	−72,474
HD 143761	HIP 78459	NSO	10,900	1,149	17,949
HD 144179	HIP 78842	NSO	10,875	436	−24,253
HD 144579	HIP 78775	NSO	11,094	1,158	−59,431
HD 144585	HIP 78955	NSO	11,112	1,158	−14,067
HD 144988	HIP 79214	NSO	11,116	1,208	−53,211
HD 145229	HIP 79165	NSO	11,100	359	−36,204
HD 145435	HIP 79152	NSO	11,086	359	−42,685
HD 145675	HIP 79248	NSO	11,307	1,150	−13,693
HD 145809	HIP 79524	NSO	11,088	1,428	21,146
HD 145897	HIP 79540	NSO	11,457	301	−23,611
HD 145934	SAO 102017	NSO	11,342	1,101	−27,954
HD 145958	HIP 79492	NSO	11,183	1,518	18,422
HD 146233	HIP 79672	NSO	11,245	1,088	11,748
HD 146362	GJ 615.2B	NSO	11,121	1,134	−14,855
HD 146775	HIP 79946	NSO	11,116	1,245	−30,218
HD 147044	HIP 79862	NSO	11,339	746	−14,560

Table 1—Continued

Primary Name	Alternate Name	Ref (NSO/M)	<JD> (−2,440,000)	ΔT (days)	<RV> (m s ^{−1})
HD 147231	HIP 79619	NSO	11,182	1,157	−16,461
HD 147379	HIP 79755	M	12,021	482	−18,789
HD 147379B	GJ 617B	M	12,040	482	−18,530
HD 147776	HIP 80366	NSO	11,541	265	7,341
HD 148467	HIP 80644	NSO	11,686	124	−36,207
HD 148513	HIP 80693	NSO	11,443	299	7,723
HD 149200	HIP 81062	NSO	11,017	22	−7,176
HD 149652	HIP 81279	NSO	11,080	359	−31,167
HD 149661	HIP 81300	NSO	10,107	3,304	−12,857
HD 149806	HIP 81375	NSO	11,358	747	10,391
HD 150433	HIP 81681	NSO	11,122	1,065	−40,215
HD 150698	HIP 81910	NSO	11,073	1,131	48,229
HD 150933	HIP 81880	NSO	11,287	747	−27,880
HD 151101	HIP 81660	NSO	11,551	455	−1,329
HD 151288	HIP 82003	M	10,162	4,746	−31,357
HD 151541	HIP 81813	NSO	11,067	1,158	9,475
HD 151877	HIP 82267	NSO	11,082	1,160	2,033
HD 151995	HIP 82389	NSO	11,145	1,429	−5,557
HD 152391	HIP 82588	NSO	10,746	2,588	45,066
HD 152446	HIP 82568	NSO	11,142	387	−42,504
HD 152792	HIP 82636	NSO	11,093	1,159	4,759
HD 153458	HIP 83181	NSO	11,258	842	641
HD 153627	HIP 83204	NSO	11,306	770	−1,462
HD 153834	HIP 83254	NSO	11,446	275	10,821
HD 154088	HIP 83541	NSO	11,071	1,131	14,180
HD 154345	HIP 83389	NSO	11,103	1,159	−46,930
HD 154363	HIP 83591	NSO	11,178	1,403	34,146
HD 154417	HIP 83601	NSO	11,331	63	−16,739
HD 155060	HIP 83827	NSO	11,175	747	−10,542
HD 155423	HIP 84082	NSO	11,367	747	−33,561
HD 156026	HIP 84478	NSO	11,367	772	153

Table 1—Continued

Primary Name	Alternate Name	Ref (NSO/M)	<JD> (−2,440,000)	ΔT (days)	<RV> (m s ^{−1})
HD 156365	HIP 84636	NSO	11,089	1,163	−13,136
HD 156681	HIP 84671	NSO	11,427	301	38,842
HD 156826	HIP 84801	NSO	11,267	1,431	−32,634
HD 157214	HIP 84862	NSO	8,668	3,650	−78,546
HD 157338	HIP 85158	NSO	11,072	1,155	−24,315
HD 157347	HIP 85042	NSO	11,256	748	−35,901
HD 157466	HIP 85007	NSO	11,399	800	34,125
HD 157617	HIP 85139	NSO	11,455	268	13,119
HD 157881	HIP 85295	M	11,130	1,427	−23,199
HD 159063	HIP 85799	NSO	11,179	699	−6,385
HD 159222	HIP 85810	NSO	11,144	1,249	−51,605
HD 159501	HIP 85888	NSO	11,470	248	−30,123
HD 159909	HIP 86193	NSO	11,212	748	−76,809
HD 160693	HIP 86431	NSO	11,076	1,157	34,084
HD 161555	HIP 86985	NSO	11,123	358	72,021
HD 161848	HIP 87089	NSO	11,064	1,428	−94,929
HD 162826	HIP 87382	NSO	11,216	625	1,848
HD 163102	HIP 87678	NSO	11,093	358	−26,920
HD 163153	HIP 87710	NSO	11,234	750	−73,024
HD 163489	GJ 4035	NSO	11,135	1,163	−49,364
HD 164507	HIP 88217	NSO	11,265	824	5,370
HD 164595	HIP 88194	NSO	11,249	748	2,020
HD 164922	HIP 88348	NSO	11,196	1,520	20,248
HD 165222	HIP 88574	M	10,299	4,747	32,671
HD 165438	HIP 88684	NSO	11,457	274	−26,747
HD 165567	HIP 88533	NSO	11,202	382	3,853
HD 165634	HIP 88839	NSO	11,394	83	−4,867
HD 165683	HIP 88636	NSO	11,426	32	−546
HD 166620	HIP 88972	NSO	9,370	3,649	−19,418
HD 167389	HIP 89282	NSO	11,254	749	−5,545
HD 168009	HIP 89474	NSO	11,329	747	−64,595

Table 1—Continued

Primary Name	Alternate Name	Ref (NSO/M)	<JD> (−2,440,000)	ΔT (days)	<RV> (m s ^{−1})
HD 168723	HIP 89962	NSO	8,930	2,734	9,371
HD 168746	HIP 90004	NSO	12,060	406	−25,603
HD 169191	HIP 90067	NSO	11,414	127	−19,268
HD 169830	HIP 90485	NSO	12,036	406	−17,304
HD 170174	SAO 123515	NSO	11,177	1,208	−28,841
HD 170469	HIP 90593	NSO	11,954	457	−59,423
HD 170493	HIP 90656	NSO	11,147	1,480	−54,752
HD 170657	HIP 90790	NSO	10,812	2,173	−43,131
HD 170778	HIP 90586	NSO	11,307	744	−22,670
HD 171067	HIP 90864	NSO	11,058	1,479	−46,252
HD 171665	HIP 91287	NSO	11,040	1,421	−23,259
HD 171918	HIP 91332	NSO	11,902	394	−67,256
HD 172051	HIP 91438	NSO	11,149	1,421	37,103
HD 172310	HIP 91381	NSO	11,189	1,038	30,997
HD 172513	HIP 91700	NSO	11,397	1,248	−11,545
HD 172649	HIP 91507	NSO	11,016	23	−11,419
HD 173701	HIP 91949	NSO	11,071	1,158	−45,602
HD 173739	HIP 91768	M	11,078	1,104	−834
HD 173740	HIP 91772	M	11,078	1,104	1,187
HD 173818	HIP 92200	NSO	11,499	443	15,544
HD 174912	HIP 92532	NSO	11,301	418	−13,083
HD 174947	HIP 92747	NSO	11,424	106	−7,100
HD 175541	HIP 92895	NSO	11,075	1,422	19,698
HD 175726	HIP 92984	NSO	11,025	44	10,277
HD 176377	HIP 93185	NSO	11,232	825	−40,611
HD 176982	HIP 93518	NSO	11,037	1,419	−6,793
HD 177153	HIP 93427	NSO	11,290	746	−14,953
HD 177830	HIP 93746	NSO	11,183	1,213	−72,173
HD 179949	HIP 94645	NSO	11,940	370	−24,662
HD 179957	GJ 9648B	NSO	11,072	1,158	−41,822
HD 179958	GJ 9648A	NSO	11,029	1,158	−41,158

Table 1—Continued

Primary Name	Alternate Name	Ref (NSO/M)	<JD> (−2,440,000)	ΔT (days)	<RV> (m s ^{−1})
HD 180617	HIP 94761	M	9,359	3,609	35,880
HD 180684	HIP 94751	NSO	11,542	420	−2,615
HD 181234	HIP 95015	NSO	11,510	451	−46,783
HD 181655	HIP 94981	NSO	11,249	897	2,036
HD 182488	HIP 95319	NSO	11,022	41	−21,508
HD 182572	HIP 95447	NSO	11,151	1,340	−100,292
HD 183341	HIP 95772	NSO	11,206	748	−40,888
HD 183650	HIP 95821	NSO	11,075	1,158	−9,744
HD 183658	HIP 95962	NSO	11,228	748	58,176
HD 183870	HIP 96085	NSO	11,295	1,517	−48,864
HD 184385	HIP 96183	NSO	11,106	441	11,406
HD 185144	HIP 96100	NSO	9,977	3,998	26,691
HD 185295	SAO 124877	NSO	11,135	1,339	−18,575
HD 185351	HIP 96459	NSO	11,426	148	−5,886
HD 185720	HIP 96813	NSO	11,027	41	15,992
HD 186408	HIP 96895	NSO	9,256	3,651	−27,377
HD 186427	HIP 96901	NSO	8,634	2,644	−27,871
HD 187123	HIP 97336	NSO	11,032	269	−16,954
HD 187237	HIP 97420	NSO	11,223	749	−32,962
HD 187897	HIP 97779	NSO	11,243	701	−37,568
HD 187923	HIP 97767	NSO	10,926	1,426	−20,611
HD 188015	HIP 97769	NSO	11,987	379	68
HD 188510	HIP 98020	NSO	11,563	452	−192,444
HD 188512	HIP 98036	NSO	8,769	3,648	−40,109
HD 189067	HIP 98206	NSO	11,119	413	−10,922
HD 189625	HIP 98589	NSO	11,268	988	−28,218
HD 190007	HIP 98698	NSO	11,225	810	−30,303
HD 190067	HIP 98677	NSO	11,009	1,517	20,385
HD 190360	HIP 98767	NSO	11,189	1,340	−45,308
HD 190404	HIP 98792	NSO	10,990	1,479	−2,527
HD 191022	HIP 98978	NSO	11,093	441	−12,842

Table 1—Continued

Primary Name	Alternate Name	Ref (NSO/M)	<JD> (−2,440,000)	ΔT (days)	<RV> (m s ^{−1})
HD 191785	HIP 99452	NSO	10,947	1,427	−49,286
HD 192020	GJ 4138	NSO	11,118	1,207	−11,366
HD 192263	HIP 99711	NSO	11,346	810	−10,738
HD 192343	HIP 99727	NSO	11,781	1,767	−526
HD 192344	HIP 99729	NSO	12,075	407	−451
HD 193017	HIP 100072	NSO	11,084	443	15,584
HD 193202	HIP 99427	NSO	11,355	26	−1,623
HD 193795	HIP 100363	NSO	11,976	369	6,921
HD 193901	HIP 100568	NSO	11,593	296	−171,455
HD 194035	HIP 100500	NSO	11,252	444	16,665
HD 194766	HIP 100895	NSO	11,101	412	−15,131
HD 195104	HIP 101059	NSO	11,022	22	−14,936
HD 195564	HIP 101345	NSO	11,141	1,428	9,535
HD 196201	HIP 101597	NSO	11,431	426	−19,821
HD 196761	HIP 101997	NSO	11,023	1,478	−41,987
HD 196850	HIP 101875	NSO	11,196	1,207	−21,045
HD 196885	HIP 101966	NSO	11,152	441	−30,189
HD 197076	HIP 102040	NSO	11,035	1,389	−35,409
HD 197139	HIP 101986	NSO	11,437	125	−24,024
HD 198089	HIP 102610	NSO	11,158	441	−33,434
HD 198802	HIP 103077	NSO	11,104	1,101	−3,171
HD 199305	HIP 103096	M	11,164	1,077	−17,161
HD 199476	HIP 102970	NSO	11,040	765	−30,230
HD 199598	HIP 103455	NSO	11,354	747	−25,301
HD 199960	HIP 103682	NSO	11,054	1,338	−17,605
HD 200538	HIP 104071	NSO	10,991	1,389	15,377
HD 200746	HIP 104075	NSO	11,408	67	13,807
HD 201091	HIP 104214	NSO	7,369	1,066	−65,726
HD 201092	HIP 104217	M	8,258	2,297	−64,023
HD 202108	HIP 104733	NSO	11,258	747	2,502
HD 202573	HIP 105000	NSO	10,823	799	−26,179

Table 1—Continued

Primary Name	Alternate Name	Ref (NSO/M)	<JD> (−2,440,000)	ΔT (days)	<RV> (m s ^{−1})
HD 202575	HIP 105038	NSO	11,175	1,337	−18,065
HD 202751	HIP 105152	NSO	11,054	1,338	−27,427
HD 203644	HIP 105497	NSO	11,436	75	−4,356
HD 204587	HIP 106147	M	11,004	1,338	−84,186
HD 206332	HIP 107040	NSO	11,254	746	−44,542
HD 206387	HIP 107107	NSO	11,807	821	−7,761
HD 206860	HIP 107350	NSO	8,929	2,894	−16,833
HD 207804	HIP 107840	NSO	10,636	63	−14,848
HD 207874	HIP 107941	NSO	11,243	720	−26,702
HD 208313	HIP 108156	NSO	11,509	335	−13,251
HD 208801	HIP 108506	NSO	10,595	2,552	−50,179
HD 209128	HIP 108691	NSO	11,432	144	8,115
HD 209290	HIP 108782	M	11,425	30	18,363
HD 209458	HIP 108859	NSO	11,586	414	−14,759
HD 209747	HIP 109068	NSO	11,404	127	−18,889
HD 209761	HIP 109023	NSO	11,443	105	−28,712
HD 209875	HIP 109144	NSO	11,208	750	−40,896
HD 210277	HIP 109378	NSO	10,756	766	−20,873
HD 210302	HIP 109422	NSO	11,472	363	−16,259
HD 210392	HIP 109428	NSO	11,972	369	−1,496
HD 210460	HIP 109439	NSO	10,843	1,093	20,429
HD 210667	HIP 109527	NSO	11,175	435	−19,443
HD 210752	HIP 109646	NSO	11,157	390	57,225
HD 210762	HIP 109602	NSO	11,438	93	−8,799
HD 211038	HIP 109822	NSO	10,807	796	10,407
HD 212801	HIP 110853	NSO	11,021	1,389	−8,475
HD 213119	HIP 110986	NSO	11,407	81	−30,288
HD 213519	HIP 111148	NSO	11,247	949	−31,630
HD 213575	HIP 111274	NSO	11,282	449	−21,544
HD 213628	HIP 111349	NSO	10,939	1,003	−50,445
HD 214557	HIP 111748	NSO	11,177	443	−38,534

Table 1—Continued

Primary Name	Alternate Name	Ref (NSO/M)	<JD> (−2,440,000)	ΔT (days)	<RV> (m s ^{−1})
HD 214749	HIP 111960	NSO	10,984	1,165	1
HD 214868	HIP 111944	NSO	11,404	128	−10,881
HD 214995	HIP 112067	NSO	11,439	93	−28,855
HD 215152	HIP 112190	NSO	11,345	783	−13,795
HD 215648	HIP 112447	NSO	8,320	1,809	−5,856
HD 216259	HIP 112870	NSO	10,981	1,517	1,291
HD 216625	HIP 113086	NSO	11,020	23	10,993
HD 216646	HIP 113084	NSO	11,435	93	−7,670
HD 216899	HIP 113296	M	11,166	1,127	−27,317
HD 217004	HIP 113386	NSO	11,015	1,072	371
HD 217014	HIP 113357	NSO	10,005	9	−33,225
HD 217107	HIP 113421	NSO	11,199	700	−13,399
HD 217165	HIP 113438	NSO	11,496	452	15,391
HD 217357	HIP 113576	M	11,087	1,074	16,420
HD 217459	HIP 113622	NSO	11,446	137	18,630
HD 217563	HIP 113686	NSO	11,448	96	4,661
HD 217618	HIP 113695	NSO	11,515	334	−12,730
HD 217813	HIP 113829	NSO	11,423	31	2,030
HD 217877	HIP 113896	NSO	11,182	442	−12,676
HD 217987	HIP 114046	M	11,139	385	8,809
HD 218029	HIP 113864	NSO	11,427	106	−8,708
HD 218133	HIP 114028	NSO	11,147	443	−48,799
HD 218209	HIP 113989	NSO	11,114	1,040	−15,895
HD 218566	HIP 114322	NSO	11,028	1,186	−37,804
HD 218730	HIP 114424	NSO	11,160	442	2,009
HD 218739	HIP 114385	NSO	11,006	0	−5,681
HD 218792	HIP 114449	NSO	11,423	105	2,548
HD 218868	HIP 114456	NSO	11,193	442	−30,622
HD 219134	HIP 114622	NSO	10,206	672	−18,558
HD 219172	HIP 114670	NSO	11,137	419	−2,828
HD 219538	HIP 114886	NSO	11,096	1,090	9,990

Table 1—Continued

Primary Name	Alternate Name	Ref (NSO/M)	<JD> (−2,440,000)	ΔT (days)	<RV> (m s ^{−1})
HD 219834B	HIP 115125	NSO	11,301	1,427	10,782
HD 219953	HIP 115194	NSO	10,989	1,517	−48,118
HD 220339	HIP 115445	NSO	11,132	1,389	34,001
HD 220957	HIP 115839	NSO	10,427	97	−81,264
HD 221146	HIP 115951	NSO	11,100	439	−15,137
HD 221354	HIP 116085	NSO	11,410	336	−25,113
HD 221356	HIP 116106	NSO	10,925	1,479	−12,713
HD 221830	HIP 116421	NSO	11,211	444	−112,299
HD 222033	HIP 116542	NSO	11,195	443	−13,088
HD 222143	HIP 116613	NSO	11,152	793	−169
HD 222368	HIP 116771	NSO	7,945	1,787	5,656
HD 222582	HIP 116906	NSO	11,315	950	12,067
HD 223238	HIP 117367	NSO	11,216	950	−15,420
HD 223498	HIP 117526	NSO	11,031	1,185	−23,985
HD 223559	HIP 117567	NSO	11,465	117	−62,839
HD 223691	HIP 117668	NSO	10,999	704	1,656
HD 223807	HIP 117756	NSO	11,483	116	−15,825
HD 224156	HIP 117953	NSO	11,482	117	14,883
HD 224383	HIP 118115	NSO	11,146	633	−31,205
HD 225216	HIP 379	NSO	11,476	117	−28,860
HD 225261	HIP 400	NSO	11,105	1,389	7,511
HD 230409	HIP 93341	NSO	11,578	346	−2,238
HD 230999	HIP 94615	NSO	11,930	335	−81,527
HD 232979	HIP 21553	M	11,693	356	34,401
HD 233641	HIP 46639	NSO	11,935	92	36,182
HD 239960	HIP 110893	M	11,146	833	−33,937
HD 245409	HIP 26335	M	11,002	1,161	22,046
HD 260655	HIP 31635	M	11,181	713	−58,178
HD 265866	HIP 33226	M	10,225	2,907	22,914
HD 281540	HIP 19143	NSO	11,515	170	110,217
HD 285968	HIP 21932	M	11,238	742	26,219

Table 1—Continued

Primary Name	Alternate Name	Ref (NSO/M)	<JD> (−2,440,000)	ΔT (days)	<RV> (m s ^{−1})
HD 349726	HIP 93873	M	11,304	723	32,407
GJ 2	HIP 428	M	12,055	405	−240
GJ 4A	HIP 473	M	11,979	405	1,669
GJ 4B	BD +45 4408B	M	12,067	432	−1,655
GJ 14	HIP 1368	M	9,537	3,745	2,957
GJ 26	G 132-11	M	12,030	608	−347
GJ 47	G 243-50	M	11,852	551	7,574
GJ 48	HIP 4856	M	11,159	866	1,500
GJ 49	HIP 4872	M	11,083	877	−5,966
GJ 54.1	HIP 5643	M	11,263	532	28,089
GJ 70	HIP 8051	M	11,867	552	−25,883
GJ 83.1	G 73-12	M	11,566	383	−28,567
GJ 96	HIP 11048	M	11,890	607	−37,941
GJ 107B	BD +48 746B	M	9,713	3,608	25,765
GJ 109	HIP 12781	M	11,522	173	30,568
GJ 156	HIP 18280	M	10,978	1,089	62,597
GJ 173	HIP 21556	M	11,788	319	−6,768
GJ 226	HIP 29277	M	11,126	741	−1,622
GJ 273	HIP 36208	M	10,129	3,167	18,216
GJ 273.1	HIP 36357	NSO	11,155	0	−3,951
GJ 357	HIP 47103	M	11,204	743	−34,581
GJ 361	HIP 47513	M	11,753	391	11,511
GJ 362	HIP 47650	M	11,777	393	6,606
GJ 373	HIP 48714	M	11,703	422	15,493
GJ 382	HIP 49986	M	11,053	974	7,932
GJ 388	SAO 81292	M	9,343	3,135	12,420
GJ 390	HIP 51007	M	11,818	428	21,590
GJ 393	HIP 51317	M	11,020	936	8,335
GJ 397	HIP 51525	M	11,323	351	21,052
GJ 402	HIP 53020	M	11,776	513	−1,042
GJ 406	G 45-20	M	11,316	380	19,482

Table 1—Continued

Primary Name	Alternate Name	Ref (NSO/M)	<JD> (−2,440,000)	ΔT (days)	<RV> (m s ^{−1})
GJ 408	HIP 53767	M	11,133	975	3,151
GJ 412A	HIP 54211	M	10,386	2,903	68,886
GJ 413.1	HIP 54532	M	11,759	456	−3,830
GJ 424	HIP 55360	M	11,796	513	60,401
GJ 433	HIP 56528	M	11,419	383	17,973
GJ 436	HIP 57087	M	11,778	513	9,607
GJ 445	HIP 57544	M	11,227	863	−111,654
GJ 447	HIP 57548	M	11,362	722	−31,087
GJ 450	HIP 57802	M	11,247	863	273
GJ 465	HIP 60559	M	11,764	455	51,174
GJ 486	HIP 62452	M	11,146	867	19,090
GJ 514	HIP 65859	M	11,085	1,158	14,556
GJ 519	HIP 66459	M	11,827	482	−14,557
GJ 528B	BD +27 2296B	NSO	11,519	369	−22,896
GJ 553.1	HIP 70975	M	11,882	520	−1,756
GJ 555	HIP 71253	M	11,496	171	−1,453
GJ 569	HIP 72944	M	9,424	1,336	−7,209
GJ 581	HIP 74995	M	11,498	176	−9,398
GJ 615.1B	BD +13 3091B	NSO	11,244	1,520	18,427
GJ 625	HIP 80459	M	11,224	842	−13,034
GJ 628	HIP 80824	M	11,759	688	−21,222
GJ 649	HIP 83043	M	12,002	780	4,316
GJ 667C	...	M	11,982	458	6,353
GJ 671	HIP 84790	M	12,056	457	−19,528
GJ 678.1A	HIP 85665	M	11,218	749	−12,457
GJ 686	HIP 86287	M	11,149	1,099	−9,515
GJ 687	HIP 86162	M	11,173	1,101	−28,779
GJ 694	HIP 86776	M	11,250	748	−14,269
GJ 699	HIP 87937	M	10,418	4,022	−110,506
GJ 729	HIP 92403	M	11,397	721	−10,499
GJ 745B	HIP 93899	M	11,304	723	32,171

Table 1—Continued

Primary Name	Alternate Name	Ref (NSO/M)	<JD> (−2,440,000)	ΔT (days)	<RV> (m s ^{−1})
GJ 793	HIP 101180	M	11,209	401	10,599
GJ 806	HIP 102401	M	9,736	4,037	−24,702
GJ 821	HIP 104432	M	12,001	430	−58,267
GJ 849	HIP 109388	M	10,972	834	−15,256
GJ 905	G 171-10	M	11,248	542	−77,949
GJ 908	HIP 117473	M	10,076	4,505	−71,147
GJ 1005	HIP 1242	M	11,044	60	−26,425
GJ 1148	HIP 57050	M	11,834	484	−9,095
GJ 2066	HIP 40501	M	11,042	744	62,205
GJ 2130A	HIP 86961	M	12,007	460	−28,990
GJ 3126	G 244-47	M	11,872	551	−84,115
GJ 3709B	...	M	11,786	426	−9,226
GJ 3804	HIP 67164	M	11,910	517	4,969
GJ 3897B	HIP 74434	NSO	11,213	1,306	−38,829
GJ 3992	HIP 84099	M	11,928	419	−44,443
GJ 4048A	G 204-58	M	11,994	458	477
GJ 4062	G 205-28	M	11,940	423	−19,003
GJ 4063	...	M	11,519	296	12,495
GJ 4070	HIP 91699	M	12,021	456	−31,764
GJ 4098	G 207-19	M	12,025	423	−1,730
GJ 4333	HIP 115332	M	12,042	229	−6,507
GJ 9492	HIP 71898	M	11,184	864	18,704
HIP 795	BD +07 9s	NSO	11,419	208	14,685
HIP 5004	G 269-87	NSO	11,865	547	45,733
HIP 10449	SAO 129772	NSO	11,481	140	28,116
HIP 15904	BD +11 468	NSO	11,668	249	86,739
HIP 52942	SAO 99310	NSO	11,425	536	24,574
HIP 59406	...	M	11,745	392	−9,100
HIP 80295	BD -11 4126	NSO	11,455	395	−17,315
HIP 89215	BD +05 3640	NSO	11,795	689	−1,050
HIP 103039	...	M	11,239	747	16,300

Table 1—Continued

Primary Name	Alternate Name	Ref (NSO/M)	<JD> (−2,440,000)	ΔT (days)	<RV> (m s ^{−1})
HIP 103269	BD +41 3931	NSO	11, 531	336	−130, 673
HIP 106924	BD +59 2407	NSO	11, 640	296	−244, 634
BD +18 4505C	...	NSO	11, 999	722	−89, 693
BD -10 3166	...	NSO	11, 499	533	26, 679
G 161-29	...	NSO	11, 448	413	22, 370
G 195-59	...	M	11, 782	401	−3, 451
G 60-06	...	NSO	11, 418	533	−18, 105

^a Stars with $\sigma_{\text{rms}} < 100 \text{ m s}^{-1}$.

Table 2. Radial Velocities:Stars with RMS > 0.1 km s⁻¹ ^a

Primary Name	Alternate Name	Ref (NSO/M)	JD (-2,440,000)	RV (m s ⁻¹)	<JD> (-2,440,000)	ΔT (days)	σ_{rms} (m s ⁻¹)	N	Com
HD 1854	SAO 192490	NSO	10984.112	24,327	10,714	119	3,651	4	
HD 3346	HIP 2900	NSO	10012.747	-33,377	9,317	2,220	172	29	
HD 3770	HIP 3169	NSO	11774.903	-8,124	11,555	1,132	178	13	L
HD 3795	HIP 3185	NSO	11756.021	-46,595	11,131	1,535	156	24	L
HD 4271	HIP 3540	NSO	11047.927	32,566	11,037	21	7,799	2	
HD 4747	HIP 3850	NSO	11756.051	10,399	11,092	1,731	315	21	CO
HD 7483	HIP 5881	NSO	12129.043	-17,717	12,015	515	2,602	11	CO
HD 8331	HIP 6442	NSO	11154.627	-12,270	11,091	128	2,349	2	
HD 9770	HIP 7372	NSO	11070.080	33,562	11,057	27	122	2	
HD 11909	HIP 9110	NSO	11438.923	-6,173	11,430	13	137	4	L
HD 14802	HIP 11072	NSO	11170.808	18,824	10,863	709	418	7	L
HD 17037	HIP 12764	NSO	11581.755	16,915	11,452	1,295	560	14	L
HD 18445	HIP 13769	NSO	11580.723	49,877	11,491	1,147	222	10	C
HD 21017	HIP 15861	NSO	11779.008	8,561	11,455	74	371	5	L
HD 25329	HIP 18915	M	11412.131	-25,177	11,179	361	338	3	
HD 25535	HIP 18824	NSO	10786.825	10,205	10,576	421	203	2	
HD 28388	HIP 20802	NSO	11170.888	17,748	10,942	457	498	6	L
HD 29461	HIP 21654	NSO	11581.849	40,518	11,763	563	116	8	L
HD 29587	HIP 21832	NSO	11073.077	111,729	10,856	610	786	4	
HD 30339	HIP 22429	NSO	12003.721	12,208	11,911	211	1,538	10	CO
HD 30649	HIP 22596	NSO	11582.778	28,904	11,391	1,545	108	14	L
HD 31412	HIP 22919	NSO	11581.861	47,494	11,317	1,062	144	12	L
HD 32387	HIP 23550	NSO	11072.132	54,468	10,759	706	1,819	3	
HD 32450	HIP 23452	M	11073.049	-11,004	10,956	233	380	2	

Table 2—Continued

Primary Name	Alternate Name	Ref (NSO/M)	JD (−2,440,000)	RV (m s ^{−1})	$\langle \text{JD} \rangle$ (−2,440,000)	ΔT (days)	σ_{rms} (m s ^{−1})	N	Com
HD 34101	HIP 24419	NSO	11073.046	33,664	10,950	1,942	2,543	7	CO
HD 35956	HIP 25662	NSO	11551.891	9,942	11,346	1,822	2,457	14	C
HD 39587	HIP 27913	NSO	10068.858	−12,171	8,846	4,580	1,294	38	CO
HD 43587	HIP 29860	NSO	11582.848	5,776	11,160	1,638	3,361	14	C
HD 50639	HIP 33109	NSO	11552.956	−2,947	11,412	1,169	207	8	L
HD 54563	HIP 34608	NSO	10784.061	−15,291	10,553	365	8,953	4	
HD 64468	HIP 38657	NSO	11581.909	−10,624	11,267	1,541	3,991	13	C
HD 65430	HIP 39064	NSO	11581.938	−28,709	11,214	1,846	470	26	CO
HD 68988	HIP 40687	NSO	12064.768	−69,520	11,919	513	120	13	C
HD 72780	HIP 42112	NSO	11626.698	28,059	11,693	412	169	10	L
HD 73512	HIP 42418	NSO	11171.030	10,737	11,199	56	29,558	2	
HD 73668	HIP 42488	NSO	11229.858	−21,456	11,270	775	112	24	L
HD 81133	HIP 45995	NSO	10546.835	11,635	10,624	400	2,456	3	
HD 86680	HIP 49060	NSO	11974.896	7,317	11,935	91	4,728	8	L
HD 89744	HIP 50786	NSO	11698.722	−5,401	11,675	737	166	45	C
HD 94340	HIP 53217	NSO	10545.893	−15,203	10,518	84	5,126	3	
HD 100167	HIP 56257	NSO	11242.931	−27,596	11,037	411	4,649	2	
HD 101206	HIP 56829	M	11551.097	40,597	11,107	945	22,398	5	C
HD 101563	HIP 57001	NSO	10955.788	−9,602	10,745	494	656	5	L
HD 102540	HIP 57574	NSO	10955.792	−4,260	10,745	494	4,055	5	L
HD 103829	HIP 58318	NSO	12101.779	−552	11,987	202	128	8	L
HD 106252	HIP 59610	NSO	11628.817	15,368	11,767	1,209	114	15	C
HD 111312	HIP 62505	NSO	11582.041	623	11,186	1,119	1,094	5	
HD 114762	HIP 64426	NSO	9858.733	49,576	9,723	4,069	434	66	C

Table 2—Continued

Primary Name	Alternate Name	Ref (NSO/M)	JD (-2,440,000)	RV (m s ⁻¹)	<JD> (-2,440,000)	ΔT (days)	σ _{rms} (m s ⁻¹)	N	Com
HD 117126	HIP 65708	NSO	11026.672	-7,637	10,975	195	1,685	5	
HD 117176	HIP 65721	NSO	9124.792	5,036	9,853	4,928	182	106	C
HD 117635	HIP 65982	NSO	10954.918	-51,998	10,752	492	336	3	
HD 120136	HIP 67275	NSO	8779.738	-16,542	9,558	5,097	340	93	C
HD 120690	HIP 67620	NSO	10606.790	7,159	10,535	144	984	2	
HD 122676	HIP 68634	NSO	11004.712	-8,017	10,955	196	1,419	3	
HD 122742	HIP 68682	NSO	10504.970	-8,081	8,986	3,545	3,712	24	CO
HD 129814	HIP 72043	NSO	11680.036	6,727	11,474	1,266	101	13	L
HD 131511	HIP 72848	NSO	9914.784	-31,806	8,966	2,866	8,832	20	CO
HD 131976	HIP 73182	M	10181.904	35,628	9,298	2,958	10,056	9	C
HD 136118	HIP 74948	NSO	11627.902	-3,062	11,660	1,326	136	40	C
HD 136580	HIP 75039	NSO	11627.962	-25,626	11,463	1,291	204	19	L
HD 140913	HIP 77152	NSO	11304.900	-18,679	10,474	1,511	742	12	CO
HD 142229	HIP 77810	NSO	11704.927	-21,443	11,660	758	486	9	L
HD 142267	HIP 77801	NSO	10603.902	35,666	10,440	328	3,931	2	
HD 145206	HIP 79195	NSO	11407.673	-36,942	11,379	53	2,180	3	
HD 152311	HIP 82621	NSO	10713.733	-21,385	10,622	166	354	3	
HD 157681	HIP 84950	NSO	11811.653	-7,723	11,449	299	133	6	
HD 158222	HIP 85244	NSO	10982.968	-14,301	11,103	413	2,698	3	
HD 160346	HIP 86400	NSO	10656.768	15,947	9,951	1,456	3,724	7	
HD 161198	HIP 86722	NSO	10666.816	23,951	10,516	391	351	3	
HD 161797	HIP 86974	NSO	11372.852	-17,004	9,872	4,324	210	53	L
HD 166435	HIP 88945	NSO	11026.782	-14,403	11,017	23	105	4	
HD 167665	HIP 89620	NSO	11702.962	7,693	11,320	1,879	322	16	L

Table 2—Continued

Primary Name	Alternate Name	Ref (NSO/M)	JD (-2,440,000)	RV (m s ⁻¹)	<JD> (-2,440,000)	ΔT (days)	σ_{rms} (m s ⁻¹)	N	Com
HD 168443	HIP 89844	NSO	11071.770	-48,636	10,976	825	182	37	C
HD 169822	HIP 90355	NSO	11793.810	-18,274	11,824	817	312	22	C
HD 171115	HIP 91004	NSO	11780.777	-2,291	11,425	106	175	5	
HD 173667	HIP 92043	NSO	8437.936	23,043	9,353	5,165	124	91	
HD 174457	HIP 92418	NSO	11755.929	-25,820	11,700	755	908	9	CO
HD 175518	HIP 92918	NSO	11014.815	-66,763	11,019	22	1,946	6	
HD 183255	HIP 95575	M	10666.899	-68,922	10,606	119	10,961	3	
HD 184860	HIP 96471	NSO	11793.808	63,944	11,373	1,845	514	21	C
HD 186704	HIP 97255	NSO	11411.863	-15,117	11,383	70	3,021	4	L
HD 188376	HIP 98066	NSO	10713.746	-39,136	10,492	430	11,891	4	
HD 190406	HIP 98819	NSO	11411.872	4,757	9,477	4,364	121	52	L
HD 190771	HIP 98921	NSO	11826.657	-25,063	11,478	1,072	136	13	L
HD 195019	HIP 100970	NSO	11792.783	-91,582	11,214	788	188	50	C
HD 197214	HIP 102264	NSO	10713.839	-21,884	10,565	437	4,096	4	
HD 199918	HIP 103735	NSO	10957.090	52,560	10,661	591	3,443	5	
HD 200565	HIP 103983	NSO	11792.788	-2,425	11,702	793	137	24	L
HD 208527	HIP 108296	NSO	10304.870	4,154	10,102	2,550	133	30	
HD 208776	HIP 108473	NSO	11440.695	31,491	11,150	435	601	10	CO
HD 209779	HIP 109110	NSO	11751.921	-17,310	11,543	335	1,722	6	L
HD 215578	SAO 108160	NSO	11439.882	-16,217	11,208	1,823	1,323	21	L
HD 217303	HIP 113562	NSO	11782.895	-36,049	11,439	96	205	7	
HD 219420	HIP 114834	NSO	11049.844	-22,295	11,027	44	2,813	5	L
HD 220077	HIP 115279	NSO	11707.121	1,521	11,727	821	132	20	
HD 223084	HIP 117258	NSO	11706.125	2,164	11,310	701	180	33	L

Table 2—Continued

Primary Name	Alternate Name	Ref (NSO/M)	JD (−2,440,000)	RV (m s ^{−1})	$\langle\text{JD}\rangle$ (−2,440,000)	ΔT (days)	σ_{rms} (m s ^{−1})	N	Com
GJ 84	HIP 9724	M	11583.710	23,335	11,419	1,294	867	11	CO
GJ 285	HIP 37766	M	11629.714	26,531	10,322	2,280	299	7	
GJ 494	HIP 63510	M	12127.800	−11,228	12,004	546	110	15	A
GJ 595	HIP 76901	M	11584.166	84,921	11,886	898	4,624	10	CO
GJ 623	HIP 80346	M	10181.925	−26,284	9,208	3,222	1,238	12	CO
GJ 873	HIP 112460	M	11447.748	413	9,714	4,401	124	17	
GJ 876	HIP 113020	M	11072.938	−1,591	10,514	4,016	181	53	C
HIP 35519	SAO 115271	NSO	11552.969	11,636	11,625	803	1,529	5	
HIP 52940	BD +13 2311B	NSO	11706.829	25,212	11,574	1,137	1,310	15	CO
HIP 57450	BD +51 1696	NSO	11679.832	64,092	11,520	810	1,211	10	
CD -32 8503B	...	NSO	11679.866	20,940	11,264	724	319	5	

^a Stars with $\sigma_{\text{rms}} \geq 100$ m s^{−1}.

Table 3. Orbital Parameters

Star	P (days)	K (km s $^{-1}$)	e	ω (deg)	T_0 (-2450000)	M_1 (M_\odot)	$M_{2,\min}$ (M_{Jup})	a_{\min} (AU)	$f(M)$ (M_\odot)	Other References
HD 4747	6832 (653)	0.65 (0.1)	0.64 (0.06)	257 (5)	453 (473)	0.83	42.3	6.7	0.000087	
HD 7483	701.42 (0.01)	3.02 (0.01)	0.12 (0.003)	313 (0.5)	1791.1 (0.7)	0.92	136	1.6	0.0020	
HD 30339	15.0778 (0.0003)	5.94 (0.01)	0.25 (0.001)	43 (1)	1881.199 (0.0003)	1.10	77.8	0.13	0.00030	
HD 34101	803.51 (0.03)	3.59 (0.01)	0.08 (0.001)	275 (1)	690 (2)	0.87	167	1.7	0.0038	
HD 39587	5136 (12)	1.85 (0.02)	0.45 (0.01)	111 (1)	1463 (17)	0.89	143	5.9	0.0024	
HD 65430	3138 (342)	1.11 (0.2)	0.32 (0.02)	77 (1)	3267 (302)	0.78	67.8	4.0	0.00038	
HD 122742	3617 (7)	6.41 (0.01)	0.48 (0.001)	183 (0.1)	2030 (3)	0.96	545	5.3	0.0670 ⁺	1,2,3,4,5
HD 131511	125.396 (0.001)	19.10 (0.01)	0.51 (0.001)	219 (0.1)	203.407 (0.004)	0.78	455	0.52	0.0580 ⁺	6,7
HD 140913	147.968 (0.001)	1.94 (0.01)	0.54 (fixed)	18 (1)	1321.42 (0.02)	0.98	43.2	0.55	0.000067 ⁺	8,9,10,11
HD 174457	840.80 (0.05)	1.25 (0.01)	0.23 (0.01)	139 (1)	2020 (4)	1.19	65.8	1.9	0.00016	
HD 208776	2624 (371)	5.46 (1.3)	0.27 (0.04)	245 (12)	690 (100)	1.24	511	4.2	0.0400	
GJ 84	6818 (2491)	2.18 (0.2)	0.44 (0.08)	238 (10)	1777 (41)	0.39	115	5.6	0.0054	
GJ 595	62.6277 (0.0001)	6.57 (0.01)	0.26 (0.001)	253 (0.1)	1999.50 (0.02)	0.28	60.0	0.22	0.0017	
GJ 623	1366.1 (0.4)	2.08 (0.04)	0.67 (0.01)	251 (1)	1298 (10)	0.31	42.0	1.7	0.00053	12,13,14,15,16,1
HIP 52940	1393.5 (0.2)	2.15 (0.01)	0.37 (0.003)	199 (1)	1541 (2)	1.12	126	2.6	0.0011	

References. — (1) Duquennoy & Mayor 1991; (2) Martin et al. 1998; (3) Blazit et al. 1987; (4) Kamper 1987; (5) Wagman 1949; (6) Beavers & Salo 1983; (7) Kamper & Lyons 1981; (8) Halbwachs et al. 2000; (9) Mazeh et al. 1996; (10) Oetiker et al. 2001; (11) Mayor et al. 1997; (12) McCarthy 1996; (13) Barbieri et al. 1996; (14) Henry & McCarthy 1993; (15) Marcy & Moore 1989; (16) McCarthy & Henry 1987; (17) Lippincott & Borgman 1978

Table 4. Stars With Linear Trends

Primary Name	Alternate Name	Slope (m s ⁻¹ per day)	N Obs
HD 3770	HIP 3169	0.41 (0.02)	13
HD 3795	HIP 3185	0.363 (0.003)	24
HD 11909	HIP 9110	23.7 (0.8)	4
HD 14802	HIP 11072	-1.73 (0.02)	7
HD 17037	HIP 12764	-1.5 (0.1)	14
HD 21017	HIP 15861	-11.3 (0.3)	5
HD 28388	HIP 20802	-2.7 (0.3)	6
HD 29461	HIP 21654	0.58 (0.02)	9
HD 30649 ^a	HIP 22596	0.27 (0.02)	15
HD 31412	HIP 22919	0.414 (0.009)	12
HD 50639	HIP 33109	-0.51 (0.01)	8
HD 72780	HIP 42112	-0.91 (0.03)	10
HD 73668	HIP 42488	-0.69 (0.02)	24
HD 86680 ^b	HIP 49060	112 (7)	8
HD 101563	HIP 57001	-3.22 (0.07)	5
HD 102540	HIP 57574	-19.9 (0.5)	5
HD 103829	HIP 58318	-2.28 (0.07)	8
HD 129814	HIP 72043	-0.224 (0.004)	13
HD 136580	HIP 75039	-0.47 (0.02)	18
HD 142229	HIP 77810	-1.47 (0.06)	9
HD 161797	HIP 86974	-0.147 (0.006)	42
HD 167665	HIP 89620	-0.59 (0.02)	16
HD 186704 ^b	HIP 97255	-88 (8)	4
HD 190406	HIP 98819	-0.066 (0.001)	58
HD 190771	HIP 98921	0.30 (0.02)	13
HD 200565	HIP 103983	-0.54 (0.01)	24
HD 209779	HIP 109110	-10.7 (0.1)	6
HD 215578	SAO 108160	-2.51 (0.03)	21
HD 219420	HIP 114834	-135.5 (0.5)	5
HD 223084	HIP 117258	-0.85 (0.04)	33

^aExhibits some additional positive curvature^bExhibits some additional negative curvature